

Brain Maturation in Adolescence and Young Adulthood: Regional Age-Related Changes in Cortical Thickness and White Matter Volume and Microstructure

Christian K. Tamnes¹, Ylva Østby¹, Anders M. Fjell^{1,2}, Lars T. Westlye¹, Paulina Due-Tønnessen³ and Kristine B. Walhovd^{1,2}

¹Center for the Study of Human Cognition, Department of Psychology, University of Oslo, 0317 Oslo, Norway,

²Department of Neuropsychology, Ullevaal University Hospital, 0407 Oslo, Norway and ³Department of Radiology, Rikshospitalet University Hospital, 0027 Oslo, Norway

The development of cortical gray matter, white matter (WM) volume, and WM microstructure in adolescence is beginning to be fairly well characterized by structural magnetic resonance imaging (sMRI) and diffusion tensor imaging (DTI) studies. However, these aspects of brain development have rarely been investigated concurrently in the same sample and hence the relations between them are not understood. We delineated the age-related changes in cortical thickness, regional WM volume, and diffusion characteristics and investigated the relationships between these properties of brain development. One hundred and sixty-eight healthy participants aged 8–30 years underwent sMRI and DTI. The results showed regional age-related cortical thinning, WM volume increases, and changes in diffusion parameters. Cortical thickness was the most strongly age-related parameter. All classes of measures showed unique associations with age. The results indicate that cortical thinning in adolescence cannot be explained by WM maturation in underlying regions as measured by volumetry or DTI. Moderate associations between cortical thickness and both volume and diffusion parameters in underlying WM regions were also found, although the relationships were not strong. It is concluded that none of the measures are redundant and that the integration of the 3 will yield a more complete understanding of brain maturation.

Keywords: cerebral cortex, cortical thinning, development, diffusion, MRI

Introduction

Total brain volume increases throughout the first years of life and then stays relatively stable. By the age of 6 years, the total size of the brain is approximately 90% of its adult size (Reiss et al. 1996; Giedd 2004). Regional maturational changes in the brain do continue throughout adolescence and into adulthood. Gray matter (GM) volume reductions appear counter-weighted by white matter (WM) increases to produce a relatively stable total volume (Rivkin 2000). Although a complex interplay between cortical and WM development is assumed, it has rarely been investigated in a detailed manner, and very little is known about this relationship. The adolescent phase of cortical thinning may reflect pruning in the form of use-dependent selective synapse elimination (Bourgeois and Rakic 1993; Huttenlocher and Dabholkar 1997; Shaw et al. 2008). This could play a key role in shaping neural circuits and thus be a biological basis for ongoing development of cognitive abilities and behavior (Hensch 2004; Knudsen 2004). Alternatively, events occurring at the interface between cortical GM and WM might at least partly explain the apparent cortical thinning during adolescence. Proliferation of myelin into the periphery of the cortical neuropil is one possible such biological event (Yakovlev and

Lecours 1967; Sowell et al. 2004; Shaw et al. 2008). This could change the MR signal in such a way that tissue in the lower cortical layers classified as GM in younger subjects would be classified as WM in older subjects. In this cross-sectional study, we report regional age-related differences in cortical thickness, WM volume, and WM diffusion parameters in a large sample of adolescents and young adults. The principal objectives of the present study were to map cortical and WM development in the same group of subjects and to investigate the relationships between cortical thickness and properties of the underlying WM in the developing brain. To reach this aim, we have used a novel approach to compare cortical thickness and WM properties in anatomically adjacent areas, minimizing inaccuracies and measurement biases due to intermodal and intersubject registration (Fjell et al. 2008).

Cortical thickness and volume have been shown to follow an inverted U-shaped developmental course with a period of initial childhood increase and a subsequent adolescent decline (Jernigan et al. 1991; Pfefferbaum et al. 1994; Reiss et al. 1996; Giedd et al. 1999; Courchesne et al. 2000; Kennedy et al. 2002; Giedd 2004; Gogtay et al. 2004; Shaw et al. 2008). The adolescent decline in thickness and volume is presumably followed by a period with slower decline and the more stable cortical dimensions of adulthood (Sowell et al. 2003; Shaw et al. 2008). Studies have also shown regional-specific patterns of cortical maturation, with different areas developing at different rates and at different times (Giedd et al. 1999; Giedd 2004; Gogtay et al. 2004; Shaw et al. 2008; Sowell et al. 2004). Cortical regions with simple laminar architecture, 3-layered allocortex, tend to show simpler developmental trajectories (linear), whereas regions with complex architecture, 6-layered isocortex, typically have more complex trajectories (cubic). Transition cortex tends to have relatively simple developmental trajectories (mix of linear and quadratic) (Shaw et al. 2008). Within isocortex, peak cortical thickness is generally attained in the primary sensory and motor areas before adjacent secondary areas and association areas. In general, maturation progresses in a posterior-to-anterior and peripheral-to-central fashion (Shaw et al. 2008).

In contrast to the mostly nonlinear and regionally specific development of the cerebral cortex, WM volume has been shown to increase in a generally linear manner throughout late childhood and adolescence, with only minor slope differences in the different lobes (Giedd et al. 1999; Paus et al. 2001; Sowell et al. 2002; Giedd 2004; Lebel et al. 2008). This volume increase seems to peak in the fourth or fifth decade of life and then steadily declines (Bartzokis et al. 2001; Sowell et al. 2003; Walhovd et al. 2005). WM consists largely of myelinated

long-distance axonal projections of neurons and is important for integration of activity between different brain areas. Histological studies have demonstrated that myelination continues well into the second and even third decades of life (Yakovlev and Lecours 1967; Benes 1989; Benes et al. 1994). Diffusion tensor imaging (DTI) indirectly provides in vivo information about tissue microstructure by utilizing random diffusion of water molecules in the brain (Le Bihan 2003). The fractional anisotropy (FA) index is a frequently used intravoxel metric characterizing degree of diffusion directionality (Pierpaoli and Basser 1996). FA is sensitive to several neurobiological features, for example, axon size, density, and organization as well as degree of myelination (Beaulieu 2002; Mori and Zhang 2006; Wozniak and Lim 2006). DTI-derived indices of WM microstructure and WM volume have recently been shown to be weakly to moderately related in a middle-aged sample (Fjell et al. 2008). In the present study, the average magnitude of water diffusion (mean diffusivity: MD), as well as axial (parallel) and radial (perpendicular) diffusion were measured in addition to FA.

Age-related increases in FA and decreases in MD during childhood, adolescence, and even early adulthood have consistently been found (Klingberg et al. 1999; Morriss et al. 1999; Mukherjee et al. 2001, 2002; Schmithorst et al. 2002; Schneider et al. 2004; Barnea-Goraly et al. 2005; Ben Bashat et al. 2005; Snook et al. 2005; Zhang et al. 2005; Schneiderman et al. 2007; Ashtari et al. 2007; Bonekamp et al. 2007; Eluvathingal et al. 2007; Giorgio et al. 2008; Qiu et al. 2008). Lebel et al. (2008) reported nonlinear age-related increases in FA and decreases in MD in major WM tracts and in selected subcortical regions in the age span 5–29 years. Generally, changes were initially rapid, then slowed and reached a plateau in late adolescence or in the twenties. Studies suggest that the age-related increase in FA in fiber tracts is primarily driven by a reduction in radial diffusion (DR), whereas axial diffusion (DA) remains relatively stable or decreases slightly (Snook et al. 2005; Giorgio et al. 2008; Lebel et al. 2008). Still, others have reported a reduction of both DR and DA in many regions but usually to a greater extent in DR (Suzuki et al. 2003; Eluvathingal et al. 2007; Qiu et al. 2008, but see Ashtari et al. 2007). Although several factors can influence DR, changes in this parameter have been shown to be related to myelination (Song et al. 2002, 2003, 2005).

To our knowledge, the only study investigating morphometric cortical and microstructural WM development in the same sample reported a negative correlation between GM density in a cluster in the right frontal lobe and FA in connected tracts in a sample of 42 adolescents (Giorgio et al. 2008). This suggests that associated age-related changes may be occurring in cortical morphometry and WM microstructure, and could be interpreted as consistent with the hypothesis that the apparent cortical thinning in adolescence is at least partly driven by increased myelination around the WM-GM border. However, synaptic pruning in this cortical region has also been shown to continue into adolescence (Huttenlocher and Dabholkar 1997). The relationship between cortical and WM maturation is still poorly understood and needs to be investigated systematically across the cerebral cortex using larger samples. In the present study, we mapped the regional maturation of cortical thickness and properties of the underlying WM in the same sample, and investigated the relations between these aspects of brain development.

Materials and Methods

Subjects

The sample was drawn from 2 ongoing longitudinal research projects at the Center for the Study of Human Cognition at the University of Oslo (Neurocognitive Development/Cognition and Plasticity through the Life-Span). The studies were approved by the Regional Ethical Committee of South Norway (REK-Sør). Written informed consent was obtained from all participants older than 12 years of age and from the parent/guardian of volunteers under 18 years of age. Oral informed consent was obtained from all participants under 12 years of age. Volunteers were recruited by newspaper advertisements and through local schools and work places. Screening interviews were conducted with all participants aged 16–30 years and with the parent/guardian of participants aged 8–19 years. Participants were required to be right-handed native Norwegian speakers in the age range 8–30 years, have normal or corrected-to-normal vision and hearing, not be under psychiatric treatment, not use medicines known to affect the central nervous system (CNS) functioning, including psychoactive drugs, and not have injury or disease known to affect CNS function, including neurological or psychiatric illness, or serious head injury. One hundred and seventy-six participants satisfied these criteria. Seven participants were excluded due to lacking or incomplete magnetic resonance imaging (MRI) data because of technical issues or that the participant did not complete the scanning session. All MR scans were subjected to a radiological evaluation by a specialist in neuroradiology (P.D.-T.), and the participants were required to be deemed free of significant injuries or conditions. One participant was excluded on this basis. For the remaining 168 participants (87 female/81 male), the mean age was 17.7 years (8.2–30.8 years, standard deviation, SD = 6.1). There was no significant correlation between age and gender ($r = 0.05$, $P = 0.513$, males coded as 0 and females coded as 1). Mean full-scale IQ, as measured by the Wechsler Abbreviated Scale of Intelligence (WASI) (Wechsler, 1999), was 110.4 (82–141, SD = 9.9). As there are no Norwegian norms available for WASI, the original US material was used. A discrepancy was observed between verbal IQ and performance IQ, indicating a recruitment bias or that these norms are not accurate for Norwegian samples because a similar discrepancy has previously also been found in adults (Westlye et al. 2009). Demographic and intellectual characteristics of the sample classified in subgroups according to age are reported in Table 1.

MR Acquisition

All imaging data were acquired using a 12-channel head coil on the same 1.5-T Siemens Avanto scanner (Siemens Medical Solutions, Erlangen, Germany). The pulse sequences used for morphometric analysis were 2 repeated 3D T1-weighted Magnetization Prepared Rapid Gradient Echo (MP-RAGE), with the following parameters: time repetition (TR)/time echo (TE)/time to inversion/FA = 2400 ms/3.61 ms/1000 ms/8°, matrix 192 × 192, field of view = 192. Each volume consisted of 160 sagittal slices with voxel sizes 1.25 × 1.25 × 1.2 mm. Scanning time for each of these sequences was 7 min, 42 s. The 2 MP-RAGEs were averaged during postprocessing to increase the signal-to-noise ratio (SNR). Primarily due to motion distortion, for 25 participants (14.9%), only one MP-RAGE was used in the analyses.

Table 1
Sample characteristics

Age	Number of females	Number of males	IQ (full scale)		Verbal IQ		Performance IQ	
			Mean	SD	Mean	SD	Mean	SD
8–11	17	19	106.5	11.0	98.3	9.0	114.6	15.5
12–15	19	18	108.2	10.7	104.0	12.3	110.4	9.6
16–19	19	16	112.1	10.5	110.1	10.9	111.2	9.9
20–23	17	16	113.1	7.5	105.2	9.3	118.8	8.5
24–30	15	12	112.9	6.5	104.5	6.1	119.8	9.0
Total	87	81	110.4	9.9	104.4	10.5	114.6	11.4

Note: Demographic and intellectual characteristics of the sample classified in subgroups according to age.

The pulse sequence used for diffusion-weighted imaging (DWI) was a single-shot twice-refocused spin echo planar imaging pulse sequence with 30 diffusion sensitized gradient directions and the following parameters: TR/TE = 8200 ms/82 ms, b value = 700 s/mm², and voxel size = 2.0 × 2.0 × 2.0 mm. This sequence is optimized to minimize eddy current-induced image distortions (Reese et al. 2003). The sequence was repeated in 2 successive runs with 10 non-diffusion-weighted images ($b = 0$) in addition to 30 diffusion-weighted images collected per acquisition. The 2 acquisitions were averaged during postprocessing to increase SNR. Each volume consisted of 64 axial slices. Total scanning time was 11 min, 21 s. In addition, a T2-weighted fluid-attenuated inversion recovery sequence was run to aid neuroradiological examination.

Morphometric Analysis

All data sets were processed and analyzed at the Center for the Study of Human Cognition, University of Oslo, with additional use of computing resources from the Titan High Performance Computing facilities (<http://hpc.uio.no/index.php/Titan>). Regional cortical thickness was estimated using FreeSurfer version 4.05 with the addition of a bug fix for WM segmentation (<http://surfer.nmr.mgh.harvard.edu/fswiki>). The cortical surface was reconstructed to measure thickness at each surface location, or vertex, using a semiautomated approach described elsewhere (Dale and Sereno 1993; Dale et al. 1999; Fischl et al. 1999a, 1999b, 2001; Fischl and Dale 2000; Salat et al. 2004; Segonne et al. 2004, 2005). Thickness measurements were obtained by reconstructing representations of the GM-WM boundary (Dale and Sereno 1993; Dale et al. 1999) and the pial surface and then calculating the distance between those surfaces at each point across the cortical mantle. This method uses both intensity and continuity information from the entire 3D MR volume in segmentation and

deformation procedures to produce representations of cortical thickness. The surface is created using spatial intensity gradients across tissue classes and is therefore not simply reliant on absolute signal intensity. The surfaces produced are not restricted to the voxel resolution of the original data and thus are capable of detecting submillimeter differences between groups (Fischl and Dale 2000). The measurement technique used here has been validated via histological (Rosas et al. 2002) as well as manual measurements (Kuperberg et al. 2003). The cortical surface was then parcellated according to procedures described by Fischl et al. (2004). Each vertex is assigned a neuroanatomical label based on 1) the probability of each label at each location in a surface-based atlas space, based on a manually parcellated training set; 2) local curvature information; and 3) contextual information, encoding spatial neighborhood relationships between labels (conditional probability distributions derived from the manual training set). By the use of this automated labeling system (Fischl et al. 2004; Desikan et al. 2006), the cortical surface was divided into 33 different gyral-based areas in each hemisphere, as shown in Figure 1A. Mean intraclass correlation between this method and manual labeling has been reported to be 0.84 across all 66 areas, with a mean distance error of less than 1 mm (Desikan et al. 2006). All labels were manually inspected for accuracy. Mean thickness was then calculated for each label.

Based on the preceding cortical parcellation, regional WM volume was calculated by a newly developed algorithm (Fjell et al. 2008; Salat et al. 2009). Each gyral WM voxel was labeled according to the surface label of the nearest cortical voxel, with a 5-mm distance limit. This yielded 33 WM areas in each hemisphere, corresponding to the 33 cortical areas, as shown in Figure 1B. In addition, we obtained the volume of deep WM, which consists of all WM voxels not assigned a cortical label.

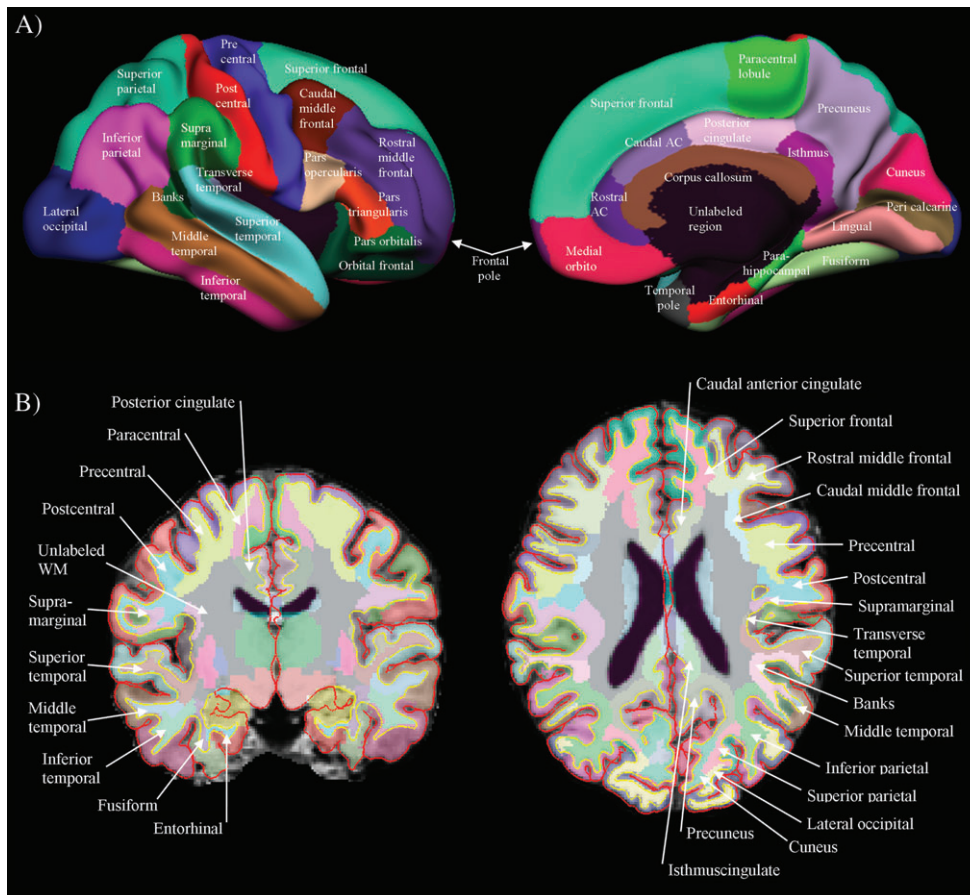


Figure 1. Automatic parcellation of the cerebral cortex and gyral WM. (A). The cortical surface was parcellated into 33 different gyral-based areas. These areas are shown for the right hemisphere in different colors on a semi-inflated average brain of the sample. The inflation procedure makes it possible to see areas buried inside the sulci that would otherwise be hidden from view. (B) Gyral WM was labeled according to the cortical parcellation of the gyri. The WM areas are shown in different colors on a representative participant (15-year-old female) in coronal and horizontal views. Some areas are not visible in these slices.

DTI Analysis

DTI processing and analyses were done using FreeSurfer and FSL (<http://www.fmrib.ox.ac.uk/fsl/index.html>). The procedure has previously been described and validated by Fjell et al. (2008). Each DTI volume was initially registered to the T2 weighted low- b ($b = 0$) image using FLIRT (Jenkinson and Smith 2001; Smith et al. 2004). This registration is a 12-parameter affine one, and accounts for both motion between scans, and for residual eddy-current distortions present in the diffusion-weighted images. Note that for the balanced echo sequences the eddy current distortions are small and the 12-parameter transformations were sufficient to remove the remaining warping. Finally, a rigid transform was computed that maximizes the mutual information between the T1-weighted anatomical and the T2-weighted low- b image. General linear modeling was used to fit the tensors to the data and create the FA and tensor maps, in addition to 3 eigenvector and eigenvalue maps. DA was defined as the principal diffusion eigenvalue (λ_1), DR as the mean of the second and third eigenvalues ($(\lambda_2 + \lambda_3)/2$) and MD as the mean of all 3 eigenvalues. In order to align the different modalities, the low- b volume was registered to each subject's anatomical volume, and the FA, eigenvector, and eigenvalue volumes were analyzed in register with the low b . The automatically generated anatomical labels from FreeSurfer were then used as masks to extract intensity information from the DTI maps. To avoid the problem of partial volume effects near the GM-WM border, each label was eroded by one voxel. Only FA values within the remaining WM label were used in the analyses. The mask lay well inside the WM volume, and the probability of GM voxels being included was thus minimized. In addition, only voxels where FA > 0.20 were included. Because each participant's DTI volumes are initially registered to the same participant's anatomical volume, the problem of spurious differences in the diffusion parameters due to imperfect intersubject registration is minimized.

In FSL, the anatomical T1 volume for each participant was linearly transformed (12 df affine registration, cost function: correlation ratio, and trilinear interpolation) into MNI152 space by the use of FLIRT (Jenkinson and Smith 2001; Smith et al. 2004). The subsequent transformation matrix was then applied to the DTI volumes and the FreeSurfer WM parcellations for each participant. Note that all volumes were initially aligned with the T1 volume before this affine registration. Next, masks based on the Mori probabilistic atlas (the Johns Hopkins University white-matter tractography atlas) provided with FSL were created, with a probability threshold of 5%. The relatively liberal probability threshold was chosen to accommodate intersubject variation in gross WM fiber architecture. The atlas contains tracts probabilistically represented in MNI space by averaging the results of deterministic tractography on 28 normal participants (Mori et al. 2005; Hua et al. 2008; Wakana et al. 2007). In this study, we investigated 9 major WM tracts in each hemisphere and 2 commissural tracts. Three-dimensional renderings of these tracts were created by the use of 3D slicer (<http://www.slicer.org/>) and are shown in Figure 2. The WM parcellations from FreeSurfer and the different tracts from the Mori atlas were simulta-

neously used as masks for the DTI volumes. For each FreeSurfer parcellation, the number of voxels overlapping with each of the Mori tracts was counted. The mean results are presented in Supplementary Figure 1. This approach made it possible to decide which major tracts contributed to each of the FreeSurfer defined WM regions for each participant. Importantly, the results are mainly consistent with those reported by Fjell et al. (2008) in a sample of participants in the age range 40-60 years. Mean intensity of all overlapping voxels from the major tracts contributing to each FreeSurfer WM region, weighted by the number of contributing voxels, was then calculated.

Statistical Analysis

Linear and quadratic effects of age on cortical thickness were calculated for both hemispheres by general linear models (GLMs) at each vertex. The vertexwise analyses were controlled for multiple comparisons using a false discovery rate (FDR) criterion. The relationships between the regional brain measures and age were investigated by regression analyses. Initial linear analyses were repeated with age² as an additional predictor variable in order to test possible quadratic components, and with age³ as a third predictor, to test for cubic components. Both uncorrected and Bonferroni-corrected P values are presented for the region of interest (ROI) analyses. Because Bonferroni corrections assume independence between variables, and the ROIs are highly correlated, this approach will, however, be too conservative. Thus, the discussion was focused on the uncorrected analyses. For those labels where age² yielded a significant contribution, exponential curves were calculated to attain better fits. As the quadratic fits generally seemed to introduce nonmonotonicity in the age relationships, exponential fits yielded more plausible description of the developmental trajectories. However, no formal statistics were performed to confirm this. We used exponential fitting equations of the form $x = b_1 + b_2 \times e^{-age/t}$, where b_1 is the estimated value at the asymptote, b_2 is the difference between the b_1 value and the estimated value at age zero, and t is a time constant indicating rate of development. Upon visual inspection, the exponential fits were deemed to represent the data well. However, more complex models could also have been investigated. For instance, in biology, allometric scaling laws have been useful in describing the relationship between 2 attributes of living organisms. A similar approach could be tested in studies of human brain maturation. Maximum development was defined as the value at the asymptote of the exponential curve (Lebel et al. 2008), and the time to reach 90% of this maximum development from the age of 8 was calculated. Absolute and relative changes from 8 to 30 years of age were calculated for all regions. Sex is known to influence absolute brain volume (Giedd et al. 1996); thus, the calculations of absolute and relative change of WM volume were done separately for males and females and averages for the merged sex groups are reported.

In order to investigate the unique contributions of the different measures, multiple regressions with age as the dependent variable and



Figure 2. Three-dimensional renderings of the probabilistic tracts. The 11 atlas-based probabilistic tracts from the Mori atlas are shown as 3D renderings in anterior, left, and dorsal views, displayed on a semitransparent template brain from FreeSurfer (fsaverage). Color codes refer to: Dark brown: Anterior thalamic radiation (ATR), Blue: Cingulum-cingulate gyrus (CCG), Purple: Cingulum-hippocampus gyrus (CHG), Dark blue: Cortico-spinal tract (CST), Pink: Forceps major (FMa), Red: Forceps minor (FMi), Brown: Inferior fronto-occipital fasciculus (IFOF), Orange: Inferior longitudinal fasciculus (ILF), Dark green: Superior longitudinal fasciculus (SLF), Green: Superior longitudinal fasciculus temporal part (SLFTP), and Yellow: Uncinate fasciculus (UF). The figure was made by the use of 3D slicer software (<http://www.slicer.org/>).

regional cortical thickness, WM volume, and FA as predictors were performed. The same procedure was repeated for MD, DA, and DR. Separate analyses were performed using FA and MD due to collinearity between these 2 parameters, because FA and MD are indexes reflecting the same diffusion eigenvalues (diffusion in either 2 or 3 directions). Including both in the same analyses would likely lead to underestimates of contributions of both parameters. Linear relationships with age were investigated for all measures in order to simplify comparisons across measures and regions. The use of linear functions in these analyses was deemed appropriate because none of the exponential fits added greatly to the amount of explained variance over the linear fits alone. Absolute and relative reductions of the squared partial β s in the multiple regressions compared with the linear regressions performed with each measure separately were calculated. Finally, correlations between cortical thickness and WM volume, FA, MD, DA, and DR were performed to test the relationships between cortical thickness and properties of the underlying WM in development.

Results

Preliminary Analyses

GLMs with cortical thickness (33 labels), WM volume, FA, MD, DA, and DR (34 labels including deep WM) in turn, and hemisphere (left, right) as within-subject contrasts, and age and gender (female, male) as between-subject contrasts yielded no significant Age \times Gender or Age \times Hemisphere interaction effects. There were no significant main effects of gender, except for on WM volume ($F[1,122] = 19.38, P = 0.0002$). Thus, in further analyses, the average of the left and right hemispheres was used. Because there were no interaction effects between gender and age for any of the measures and no main effects of gender except on WM volume, where gender was regressed out prior to further analyses, males and females were combined in all analyses. Combining males and females and measures from both hemispheres has been done in many previous developmental studies to simplify interpretation and

improve confidence in curve fits (Sowell et al. 2003; Barnea-Goraly et al. 2005; Snook et al. 2005; Lebel et al. 2008).

The results from the regression analyses with age and with age and age² as predictor variables on cortical thickness, WM volume, FA, MD, DA, and DR are reported in Supplementary Tables 1–6. The results from the regression analyses with age³ as an additional predictor variable showed few and small additional contributions of age³. In the analyses with cortical thickness, the only region with a significant contribution of age³ was the lateral orbitofrontal cortex ($P = 0.046$). The results from the analyses with age³ are therefore not reported.

Cortical Thickness

The vertexwise effects of age on cortical thickness across the surface were computed by GLM, and the results are shown in Figure 3. When a commonly used statistical threshold taking multiple comparisons into account was used (FDR < 0.05), negative linear effects were observed across almost the entire cortical mantle (Fig. 3A). When a more conservative threshold was used ($P < 10^{-12}$), strong negative effects were observed in large areas in the parietal lobes and in the superior medial frontal lobes (Fig. 3B). Strong effects were also evident bilaterally in the posterior cingulate, isthmus cingulate, lateral occipital, and ventrolateral prefrontal cortices. There were also quadratic effects, predominantly in the parietal lobes including posterior areas toward the occipital lobes (Fig. 3C). Cortical thinning was most pronounced in young age and then decelerated. The continuous absolute change in cortical thickness from 8 to 30 years is shown in Supplementary Movie 1.

The parcellation-based regional analyses confirmed the results of the vertexwise analyses, and significant negative linear effects of age on cortical thickness were found in all 33 regions, except for the entorhinal cortex and the temporal pole (Supplementary Table 1). For 21 of the 33 regions, age² added

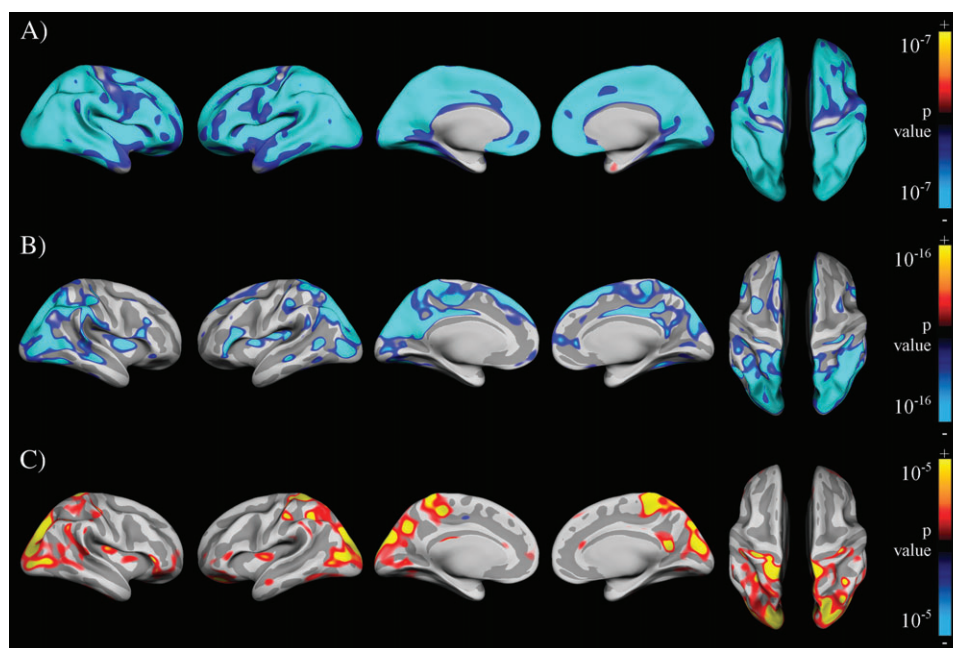


Figure 3. Effects of age on cortical thickness at each vertex. The significance of the effect is color coded and projected onto a semi-inflated average template brain. (A) Linear relationships with an FDR-corrected significance level. (B) Linear relationships with a more conservative significance level. (C) Quadratic relationships with an FDR-corrected significance level.

significantly to the amount of explained variance, and an exponential curve was fitted to the data. All the exponential fits showed thinning occurring rapidly initially, then slowing down at higher age. Using the Bonferroni-corrected *P* values, the same 31 regions showed significant negative linear effects of age and age² added significantly to the amount of explained variance in 15 regions. Explained variance of the exponential and linear fits of age on cortical thickness for each label, as well as the time constant and age at 90% of peak for the exponential fits, are shown in Table 2. The developmental timing of the cortical thinning could only be calculated for regions with an exponential fit and the estimated age at 90% of peak exceeded the age range of the sample for many of the regions, for example, the medial orbitofrontal cortex and lateral regions in the inferior parietal lobe. Among the regions that reached 90% of their minimum cortical thickness earliest (i.e., before age 25) were the lateral occipital cortex and regions in the lateral orbitofrontal cortex. Absolute change from 8 to 30 years ranged from -0.26 mm in the parahippocampal cortex to -0.66 mm in the inferior parietal cortex (see Table 2). Relative change in each region is visualized in Figure 4. The largest changes were seen laterally and medially in the parietal lobe with thickness decreases of 20% or more. Decreases of 15% or more were additionally found in the medial and superior frontal

cortex, the cingulum, postcentral cortex, and the occipital lobe. Smaller relative changes were observed in the temporal lobe, in the lateral frontal and precentral cortices.

WM Volume

There were significant positive linear effects of age on WM volume (with gender regressed out) in all regions, except the frontal pole and the caudal and rostral anterior cingulate (Supplementary Table 2). For 12 of the 34 regions, age² gave a significant contribution to the amount of explained variance, and an exponential curve was thus fitted, showing rapid increase at young age, followed by slower increase toward adulthood. With the Bonferroni-corrected *P* values, there were significant linear effects of age in 25 regions and age² only gave a significant contribution to the amount of explained variance in the precentral and the temporal pole regions. Explained variance of the exponential and linear fits of age on WM volume in each region, as well as the time constant and age at 90% of peak for the exponential fits, are shown in Table 2, and relative increases in volume are shown in Figure 4. Increases in volume of 15% or more were observed in most regions over the age span studied. The largest relative increase was observed for deep WM, which increased with 58% from 8 to 30 years.

Table 2
Age-related change in cortical thickness and WM volume

Region	Cortical thickness					WM volume				
	<i>R</i> ^{2a}	<i>t</i> ^b	Age at 90% of peak ^b	Absolute change (mm)	Percent change	<i>R</i> ^{2a}	<i>t</i> ^b	Age at 90% of peak ^b	Absolute change ^c (mm ³)	Percent change ^c
Banks superior temporal sulcus	<u>0.44</u>	11.03	33.38	-0.46	-15.08	<u>0.06</u>			440.96	15.12
Caudal anterior cingulate	<u>0.26</u>			-0.46	-15.30	<u>0.04</u>	2.08	12.79	275.02	12.60
Caudal middle frontal	<u>0.39</u>			-0.37	-12.88	<u>0.15</u>	2.05	12.72	1843.43	36.48
Cuneus	<u>0.57</u>	7.74	25.82	-0.53	-22.83	<u>0.17</u>	3.61	16.30	810.97	36.53
Entorhinal	<u>0.01</u>			0.11	3.11	<u>0.06</u>			145.96	24.66
Fusiform	<u>0.46</u>	10.10	31.27	-0.35	-11.45	<u>0.20</u>	4.67	18.76	1619.04	31.27
Inferior parietal	<u>0.68</u>	11.89	35.39	-0.66	-21.45	<u>0.07</u>			1505.88	14.37
Inferior temporal	<u>0.44</u>	8.05	26.53	-0.40	-11.97	<u>0.08</u>			971.24	16.92
Isthmus cingulate	<u>0.48</u>	10.14	31.33	-0.56	-17.33	<u>0.03</u>			220.87	8.53
Lateral occipital	<u>0.59</u>	7.05	24.22	-0.51	-18.80	<u>0.13</u>	3.23	15.44	2189.74	23.09
Lateral orbitofrontal	<u>0.39</u>	6.46	22.88	-0.41	-13.11	<u>0.19</u>	3.76	16.67	1456.64	22.94
Lingual	<u>0.52</u>	9.82	30.61	-0.36	-15.30	<u>0.12</u>			946.49	16.64
Medial orbitofrontal	<u>0.42</u>	13.56	39.16	-0.47	-16.30	<u>0.05</u>			373.23	11.27
Middle temporal	<u>0.50</u>	10.13	31.32	-0.44	-12.95	<u>0.05</u>			690.37	11.17
Parahippocampal	<u>0.06</u>			-0.26	-9.14	<u>0.09</u>			222.28	15.87
Paracentral	<u>0.60</u>	9.76	30.48	-0.57	-20.01	<u>0.13</u>	3.58	16.25	940.72	26.41
Pars opercularis	<u>0.42</u>			-0.40	-13.39	<u>0.12</u>			772.80	20.81
Pars orbitalis	<u>0.33</u>	5.66	21.02	-0.48	-14.91	<u>0.10</u>			213.84	21.83
Pars triangularis	<u>0.48</u>	12.60	37.01	-0.43	-14.84	<u>0.08</u>			619.56	19.48
Pericalcarine	<u>0.45</u>	8.88	28.43	-0.31	-17.47	<u>0.03</u>			438.11	12.24
Postcentral	<u>0.54</u>	9.05	28.85	-0.43	-17.85	<u>0.18</u>			1494.57	20.56
Posterior cingulate	<u>0.54</u>			-0.48	-16.26	<u>0.06</u>	3.24	15.46	429.01	10.96
Precentral	<u>0.31</u>			-0.29	-10.42	<u>0.32</u>	4.57	18.52	4237.79	41.87
Precuneus	<u>0.66</u>	10.20	31.49	-0.58	-20.17	<u>0.16</u>			1878.43	20.70
Rostral anterior cingulate	<u>0.41</u>			-0.57	-16.94	<u>0.01</u>			117.18	6.47
Rostral middle frontal	<u>0.48</u>	10.10	31.27	-0.39	-14.25	<u>0.07</u>			1684.51	13.68
Superior frontal	<u>0.56</u>			-0.48	-15.12	<u>0.18</u>			3588.69	21.03
Superior parietal	<u>0.67</u>	8.85	28.37	-0.65	-23.80	<u>0.19</u>			2603.26	22.76
Superior temporal	<u>0.35</u>			-0.33	-10.54	<u>0.22</u>	5.71	21.14	1994.94	27.14
Supramarginal	<u>0.60</u>	15.07	42.70	-0.52	-17.00	<u>0.11</u>			1375.77	15.81
Frontal pole	<u>0.28</u>	7.75	25.84	-0.49	-14.61	<u>0.00</u>			-5.58	-1.39
Temporal pole	<u>0.01</u>			0.09	2.27	<u>0.26</u>	6.03	21.89	235.11	47.30
Transverse temporal	<u>0.21</u>			-0.37	-13.91	<u>0.08</u>			135.69	11.08
Deep WM						<u>0.33</u>	7.55	25.38	14840.42	57.99

Note: Explained variance (*R*²) of the exponential and linear fits, time constant (*t*) indicating the rate of development and age at 90% of peak of the exponential fits, as well as absolute and relative change of cortical thickness and WM volume (with gender regressed out) over the age span 8–30 years.

^a Explained variance is reported for the exponential fits where age² had a significant contribution and for the linear fit for the other regions. Underlined characters indicate Bonferroni-corrected *P* values < 0.05 for the quadratic or linear model.

^b *t* and age at 90% of peak is not reported for regions with a linear fit.

^c Absolute and relative change of WM volumes were calculated separately for females and males, averages for the merged sex groups are reported.

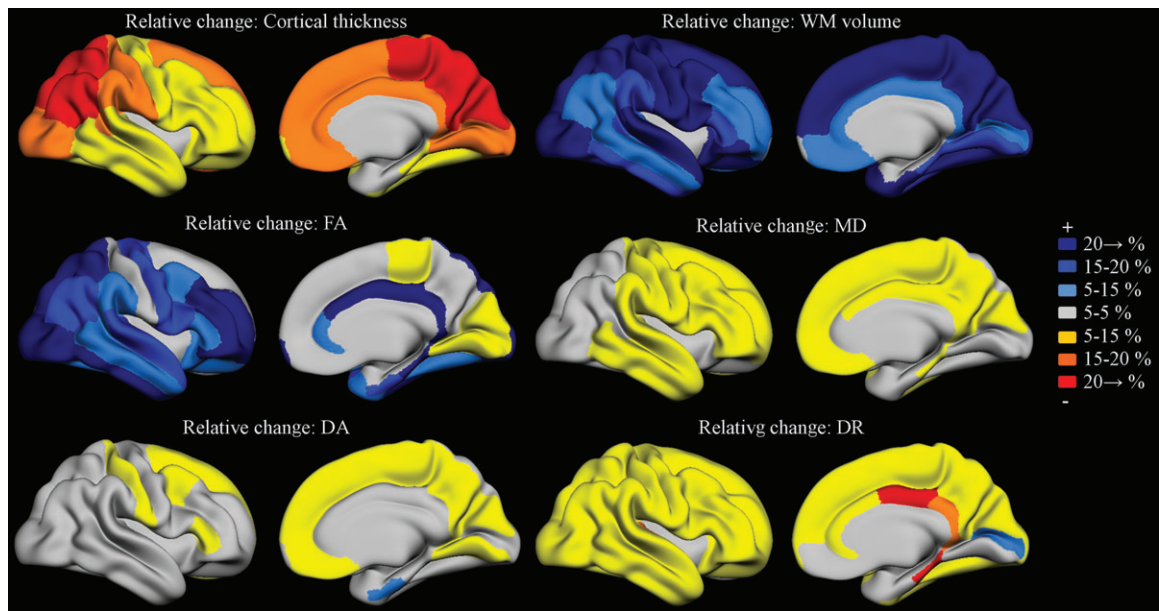


Figure 4. Relative magnitude of developmental changes over the age span 8–30 years. Percentage change of cortical thickness, WM volume (with gender regressed out), FA, MD, DA, and DR are color coded and projected onto the surface of a semi-inflated average template brain. Diffusion measures are derived from voxels in underlying WM regions that overlapped with major tracts. All measures are averages between both hemispheres. The medial wall and corpus callosum are masked out.

DTI

For FA, significant linear increases were found in 24 regions, whereas significant linear decreases were found in 5 regions in the medial posterior part of the brain (Supplementary Table 3). For 26 of the 34 labels, age^2 gave a significant contribution, and the exponential curves showed that FA increased rapidly initially, and then slowed down at higher age. Using the Bonferroni-corrected P values, significant linear increases were found in 22 regions, whereas linear decreases were found in 3 regions and age^2 gave a significant contribution in 19 regions. For MD, significant linear decreases were found in 25 regions, and age^2 gave a significant contribution in 30 of the 34 regions (Supplementary Table 4). The exponential curves showed that MD decreased most rapidly at younger age and more slowly at older age. With the Bonferroni-corrected P values, significant linear decreases were found in 22 regions and age^2 gave a significant contribution in 16 regions. Explained variance of the exponential and linear fits of age on FA and MD for each region, as well as the time constant and age at 90% of peak for the exponential fits, are shown in Table 3. Analysis of the eigenvalues revealed age-related decreases in both DA and DR, but to a larger degree in DR in terms of number of regions that showed decrease and the size of the effects. For DA we found significant linear decreases in 15 regions and increases in 6 regions (Supplementary Table 5). There were significant contributions of age^2 in 11 regions, all showing rapid decreases at younger age and slower at higher age. With Bonferroni-corrected P values, DA showed significant linear decreases in 11 regions and increases in 4 regions and age^2 gave a significant contribution in 4 regions. For DR, we found significant linear decreases in 25 regions and increase in one region (Supplementary Table 6). Significant contributions of age^2 were found in 30 regions, all showing most rapid decreases at younger age. Using Bonferroni-corrected P values, DR had linear decreases in 24 regions and age^2 had a significant

contribution in 23 regions. Explained variance of the exponential and linear fits of age on DA and DR for each region is shown in Table 4.

The relative magnitude of the changes in FA, MD, DA, and DR are visualized in Figure 4. For FA, there were increases of 20% or more in regions on the lateral side of the occipital, parietal, and frontal lobes, as well as in the cingulum, the parahippocampus, and the inferior temporal lobe. There were also moderate increases medially in the parietal and occipital lobes. For MD, there were decreases in the range of 5–13% in most regions in the frontal and temporal lobes, as well as medially in the parietal lobe. DA showed decreases in the range of 5–8% primarily medially in the frontal and parietal lobes, as well as in superior lateral regions in the frontal lobe. DR showed widespread decreases in the range of 5–15% and some larger decreases in the cingulum, the parahippocampal and the transverse temporal gyri. The developmental timing of FA and MD in all regions with an exponential fit is shown in Figure 5. By age 20, most tracts in parietal and occipital WM regions had reached 90% of their maximum FA and minimum MD. At age 23, lateral temporal regions and some frontal regions had still not reached their plateau. Some regions also appeared to continue to undergo changes in terms of both FA and MD (parahippocampal) or only in MD (medial orbitofrontal and rostral middle frontal areas) beyond 30 years of age. Scatter plots of cortical thickness, WM volume, FA, and MD by age for 5 selected regions are shown in Figure 6. The regions were selected to be representative of different parts of the cerebrum and for the overall results across regions.

Testing of Unique Effects of Cortical Thickness, WM Volume, and Diffusion Parameters

The results from the multiple regressions with age predicted from cortical thickness, WM volume, and FA as simultaneous independent variables are shown in Table 5. For 14 of the 33

Table 3
Age-related change in FA and MD

Region	FA					MD				
	R^2 ^a	t ^b	Age at 90% of peak ^b	Absolute change (FA)	Percent change	R^2 ^a	t ^b	Age at 90% of peak ^b	Absolute change (10^{-5} mm ² /s)	Percent change
Banks superior temporal sulcus	0.19	7.05	24.23	0.06	12.74	0.11	4.17	17.59	-3.43	-4.24
Caudal anterior cingulate	<u>0.22</u>	6.10	22.04	0.08	20.27	<u>0.11</u>	4.55	18.48	-4.33	-5.06
Caudal middle frontal	<u>0.18</u>	5.43	20.51	0.04	11.68	<u>0.34</u>	5.51	20.67	-8.88	-10.83
Cuneus	<u>0.03</u>			-0.02	-6.19	<u>0.07</u>	1.15	10.66	-6.03	-7.02
Entorhinal	0.11	5.47	20.60	0.05	16.20	0.01			1.43	1.67
Fusiform	<u>0.11</u>	6.10	22.05	0.04	10.85	<u>0.09</u>	6.09	22.03	-3.52	-4.29
Inferior parietal	<u>0.36</u>	6.31	22.53	0.07	17.31	<u>0.08</u>	3.43	15.89	-2.87	-3.57
Inferior temporal	<u>0.44</u>	6.96	24.03	0.10	28.47	<u>0.30</u>	8.62	27.84	-6.15	-7.51
Isthmus cingulate	<u>0.37</u>	7.24	24.67	0.10	24.49	<u>0.17</u>	5.80	21.34	-4.38	-5.56
Lateral occipital	<u>0.30</u>	5.17	19.89	0.06	20.21	<u>0.05</u>	1.12	10.58	-3.72	-4.44
Lateral orbitofrontal	<u>0.22</u>	6.00	21.82	0.05	12.63	<u>0.15</u>	6.24	22.38	-3.79	-4.65
Lingual	<u>0.12</u>			-0.05	-10.89	<u>0.01</u>			-1.76	-2.06
Medial orbitofrontal	<u>0.02</u>			-0.01	-3.05	<u>0.26</u>	12.75	37.37	-5.41	-6.52
Middle temporal	0.17	7.06	24.27	0.05	13.17	<u>0.28</u>	7.47	25.20	-5.27	-6.36
Parahippocampal	<u>0.42</u>	11.63	34.78	0.14	44.58	<u>0.28</u>	11.84	35.25	-10.17	-12.05
Paracentral	<u>0.06</u>			-0.03	-6.51	<u>0.11</u>	2.19	13.05	-4.64	-5.83
Pars opercularis	<u>0.34</u>	5.31	20.22	0.06	17.59	<u>0.35</u>	5.59	20.87	-6.62	-8.22
Pars orbitalis	<u>0.25</u>	4.79	19.04	0.06	20.78	<u>0.29</u>	5.86	21.49	-7.33	-8.63
Pars triangularis	<u>0.21</u>	4.12	17.48	0.04	12.94	<u>0.34</u>	5.90	21.59	-7.53	-9.18
Pericalcarine	<u>0.12</u>			-0.05	-12.16	<u>0.01</u>			1.74	1.93
Postcentral	<u>0.04</u>			0.01	4.01	<u>0.19</u>	4.25	15.92	-8.41	-9.98
Posterior cingulate	<u>0.37</u>	6.00	21.82	0.14	39.36	<u>0.23</u>	5.60	20.91	-8.68	-10.37
Precentral	<u>0.48</u>	4.45	18.26	0.07	18.97	<u>0.41</u>	5.11	19.76	-7.93	-9.59
Precuneus	<u>0.04</u>			-0.02	-4.18	<u>0.14</u>	3.57	16.21	-5.19	-6.17
Rostral anterior cingulate	0.05	5.67	21.06	0.04	9.60	<u>0.08</u>	4.29	17.87	-3.44	-3.99
Rostral middle frontal	<u>0.52</u>	7.06	24.27	0.06	20.70	<u>0.37</u>	10.96	33.25	-5.35	-6.37
Superior frontal	<u>0.00</u>			0.00	-0.02	<u>0.29</u>	8.16	26.80	-5.15	-6.30
Superior parietal	<u>0.39</u>	5.15	19.85	0.08	21.91	<u>0.10</u>	1.88	12.34	-3.89	-4.79
Superior temporal	<u>0.29</u>	8.10	26.66	0.06	15.84	<u>0.25</u>	7.61	25.51	-5.56	-6.51
Supramarginal	<u>0.15</u>	4.59	18.57	0.03	7.93	<u>0.21</u>	3.36	15.73	-5.16	-6.43
Frontal pole	<u>0.07</u>	2.03	12.68	0.09	40.29	<u>0.02</u>	1.59	11.66	-11.25	-12.68
Temporal pole	<u>0.01</u>	1.30	10.98	0.02	5.17	<u>0.01</u>			1.74	2.00
Transverse temporal	<u>0.11</u>	9.08	28.90	0.08	15.56	<u>0.21</u>	8.82	28.30	-9.21	-11.05
Deep WM	<u>0.05</u>	3.18	15.31	0.02	4.33	<u>0.04</u>	3.46	15.95	-1.94	-2.39

Note: Explained variance (R^2) of the exponential and linear fits, time constant (t) indicating the rate of development and age at 90% of peak of the exponential fits, as well as absolute and relative change of FA and MD over the age span 8-30 years.

^a Explained variance is reported for the exponential fits where age² had a significant contribution and for the linear fit for the other regions. Underlined characters indicate Bonferroni-corrected P values < 0.05 for the quadratic or linear model.

^b t and age at 90% of peak are not reported for regions with a linear fit.

regions, all 3 measures gave unique contributions ($P < 0.05$), whereas at least 2 of the measures gave significant contributions in 28 of the regions. Cortical thickness gave a unique significant contribution in all regions, except the parahippocampal region and the temporal pole, whereas WM volume and FA gave significant contributions in 18 and 25 of the 33 regions, respectively. Of the 3 classes of measures, cortical thickness had the largest standardized partial β value for all regions except entorhinal cortex, parahippocampal cortex, and the temporal pole. Standardized partial β s were larger for FA than for WM volume in 22 of the 33 regions. Compared with the linear regressions performed with each measure separately (Supplementary Tables 1-3), the reductions in the squared partial β s were quite similar for all 3 measures in the multiple regressions (median reduction of squared partial β for all 33 regions: cortical thickness = 0.09, WM volume = 0.07, and FA = 0.08). The median percentage reduction of the squared partial β s in all 33 regions was thus much smaller for cortical thickness (22%), than for WM volume (78%) and FA (68%).

The same procedure was repeated using MD instead of FA. The results from the multiple regressions on age with cortical thickness, WM volume, and MD as independent variables are shown in Table 6. At least 2 of the measures gave unique

contributions in most of the regions, and cortical thickness had the largest standardized β value in 30 of the 33 regions. Compared with the linear regressions performed with each measure separately (Supplementary Tables 1, 2, and 4), the reductions in the squared partial β s were slightly larger for cortical thickness than for the 2 other measures in the multiple regressions (median reductions of squared partial β s for all 33 regions: cortical thickness = 0.10, WM volume = 0.07, and MD = 0.07). The median percentage reduction of the squared partial β s was much smaller for cortical thickness (19%), than for WM volume (75%) and MD (67%). Multiple regressions on age with cortical thickness, WM volume, and DA and DR, respectively, are shown in Supplementary Tables 7 and 8.

Associations between Cortical Thickness, WM Volume, and Diffusion Parameters

Pearson correlations between cortical thickness in each region and WM volume, FA, MD, DA, and DR are shown in Table 7. Cortical thickness correlated negatively with WM volume in 24 of the 33 regions, with a median correlation for all regions of $r = -0.26$. The strongest associations were found in the lateral orbitofrontal ($r = -0.47$) and superior frontal ($r = -0.45$) regions. For FA, we found negative correlations with cortical thickness in

Table 4

Age-related change in DA and DR

Region	DA					DR				
	R^{2a}	t^b	Age at 90% of peak ^b	Absolute change (10^{-5} mm ² /s)	Percent change	R^{2a}	t^b	Age at 90% of peak ^b	Absolute change (10^{-5} mm ² /s)	Percent change
Banks superior temporal sulcus	0.00			1.03	0.85	0.18	5.50	20.66	-5.24	-8.70
Caudal anterior cingulate	0.02			2.62	2.12	<u>0.19</u>	5.23	20.03	-7.75	-11.62
Caudal middle frontal	<u>0.26</u>	6.03	21.89	-9.35	-8.17	<u>0.31</u>	5.27	20.14	-8.65	-13.15
Cuneus	<u>0.08</u>	2.55	13.86	-7.22	-6.00	<u>0.03</u>	0.93	10.15	-4.76	-7.01
Entorhinal	0.05			6.09	5.33	0.00			-0.90	-1.26
Fusiform	0.00			-0.37	-0.32	<u>0.18</u>	5.96	21.71	-5.02	-7.87
Inferior parietal	<u>0.07</u>			3.41	3.00	<u>0.22</u>	4.73	18.89	-5.48	-8.67
Inferior temporal	0.00			1.01	0.89	<u>0.46</u>	7.56	25.40	-9.91	-14.91
Isthmus cingulate	<u>0.06</u>			5.48	4.65	<u>0.38</u>	6.40	22.74	-9.07	-15.21
Lateral occipital	<u>0.10</u>			4.69	4.23	<u>0.19</u>	2.98	14.85	-5.34	-7.79
Lateral orbitofrontal	0.00			0.42	0.35	<u>0.22</u>	6.17	22.21	-5.90	-9.40
Lingual	<u>0.07</u>			-9.28	-7.23	<u>0.02</u>			2.02	3.15
Medial orbitofrontal	<u>0.33</u>	11.10	33.57	-9.95	-8.04	<u>0.08</u>			-3.04	-4.88
Middle temporal	<u>0.05</u>			-2.97	-2.54	<u>0.27</u>	6.75	23.53	-6.47	-9.87
Parahippocampal	0.00			-0.20	-0.17	<u>0.41</u>	11.49	34.46	-15.10	-21.70
Paracentral	<u>0.18</u>	7.87	26.11	-9.07	-7.32	<u>0.02</u>	0.98	10.25	-3.69	-6.40
Pars opercularis	<u>0.08</u>	5.37	20.36	-3.71	-3.31	<u>0.39</u>	5.65	21.02	-8.07	-12.46
Pars orbitalis	<u>0.06</u>			-3.98	-3.55	<u>0.33</u>	5.49	20.65	-8.79	-12.43
Pars triangularis	<u>0.22</u>	8.16	26.79	-6.67	-6.00	<u>0.34</u>	5.22	20.02	-7.99	-11.97
Pericalcarine	<u>0.02</u>			-3.70	-2.78	<u>0.04</u>			4.47	6.53
Postcentral	<u>0.16</u>	3.88	16.94	-6.72	-5.93	<u>0.19</u>	4.56	18.51	-4.75	-7.28
Posterior cingulate	<u>0.03</u>			3.65	3.10	<u>0.36</u>	5.63	20.95	-15.02	-22.31
Precentral	<u>0.16</u>	6.82	23.70	-5.04	-4.37	<u>0.48</u>	4.69	18.80	-9.44	-14.22
Precuneus	<u>0.18</u>	6.45	22.84	-8.82	-6.54	<u>0.05</u>	2.47	13.69	-3.58	-6.13
Rostral anterior cingulate	0.00			0.18	0.14	<u>0.08</u>	4.96	19.41	-4.95	-7.45
Rostral middle frontal	0.05			-1.94	-1.73	<u>0.47</u>	8.81	28.28	-7.21	-10.29
Superior frontal	<u>0.40</u>	8.99	28.70	-8.61	-7.21	<u>0.13</u>	7.38	25.00	-3.43	-5.45
Superior parietal	<u>0.08</u>			4.20	3.77	<u>0.28</u>	3.28	15.55	-6.33	-9.68
Superior temporal	<u>0.01</u>			-0.99	-0.82	<u>0.33</u>	7.56	25.41	-7.76	-11.54
Supramarginal	<u>0.08</u>	2.56	13.90	-4.10	-3.58	<u>0.24</u>	3.73	16.59	-5.74	-9.06
Frontal pole	0.00			2.09	2.13	<u>0.03</u>	1.71	11.93	-11.51	-14.61
Temporal pole	0.00			-0.02	-0.02	0.00	1.37	11.16	-1.79	-2.50
Transverse temporal	<u>0.06</u>			-6.36	-4.85	<u>0.18</u>	8.64	27.89	-10.41	-17.72
Deep WM	<u>0.01</u>			-1.03	-0.84	<u>0.05</u>	2.88	14.63	-2.48	-4.15

Note: Explained variance (R^2) of the exponential and linear fits, time constant (t) indicating the rate of development and age at 90% of peak of the exponential fits, as well as absolute and relative change of axial (DA) and radial (DR) diffusion over the age span 8–30 years.

^a Explained variance is reported for the exponential fits where age² had a significant contribution and for the linear fit for the other regions. Underlined characters indicate Bonferroni-corrected P values < 0.05 for the quadratic or linear model.

^b t and age at 90% of peak are not reported for regions with a linear fit.

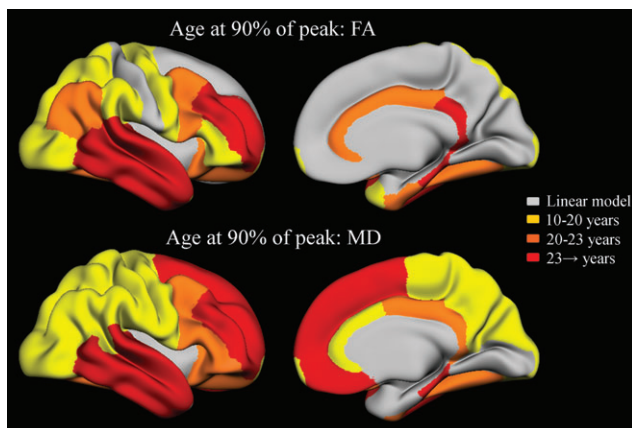


Figure 5. Timing of developmental changes in FA and MD. The age at which the region reached 90% of its developmental peak from 8 years, as measured by fitting parameters in the exponential equation, is color coded and projected onto the surface of a semi-inflated average template brain. Measures are derived from voxels in underlying WM regions that overlapped with major tracts. All measures are averages between both hemispheres. Timing of developmental changes could not be calculated in regions with a linear fit. The medial wall and corpus callosum are masked out.

22 regions and positive correlations in 4 regions in the medial posterior part of the brain. The median correlation between cortical thickness and FA for all regions was $r = -0.23$. MD and

cortical thickness correlated positively in 22 regions and negatively in one (pericalcarine). The median correlation was $r = 0.25$.

Correlations between WM volume and the diffusion measures in each region are shown in Supplementary Table 9. In short, there were fewer and smaller significant correlations between WM volume and the diffusion parameters, than between the different WM measures and cortical thickness. Of the 34 regions (including deep WM) WM volume showed significant positive correlations with FA in 13 regions and negative correlations with MD in 12 regions. Partial correlations between the different measures when controlled for age are shown in Supplementary Tables 10 and 11. In summary, these showed the same general tendencies as the bivariate correlations reported above, although the effect sizes were substantially reduced.

Discussion

The present study shows regional age-related cortical thinning, WM volume increases and changes in diffusion parameters in major WM tracts. Cortical thinning was observed across almost the entire cortical mantle in a vertex-by-vertex analysis and in nearly all regions. In the majority of regions, cortical thickness decreased nonlinearly, with the greatest change occurring in adolescence. Percentage decrease in thickness was largest in the

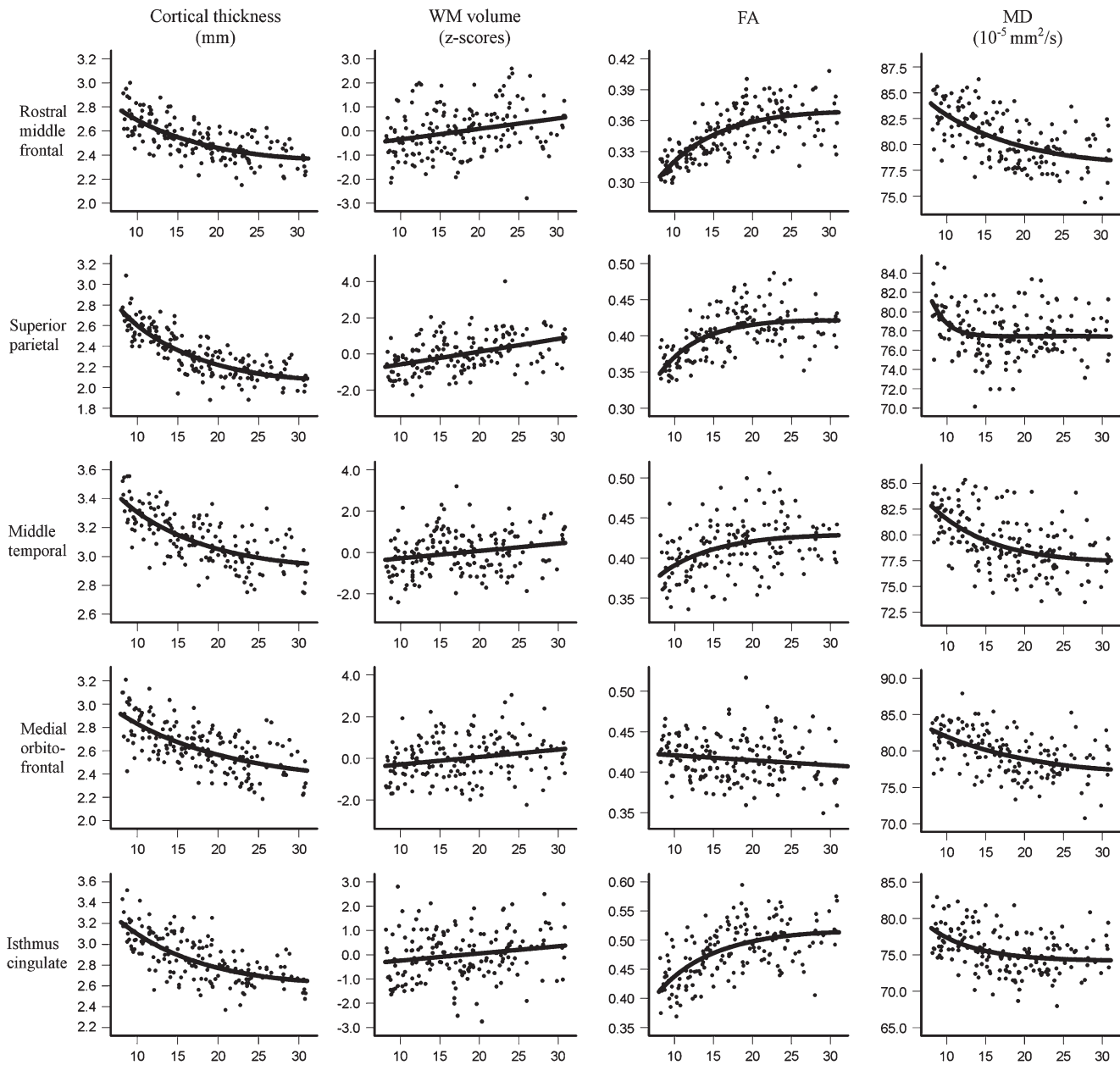


Figure 6. Scatter plots for, columnwise from left to right: cortical thickness, WM volume, FA, and MD by age (in years) for 5 selected representative regions. The regions for which age-related changes are shown are from top to bottom: rostral middle frontal, superior parietal, middle temporal, medial orbitofrontal, and isthmus cingulate. For most regions, age-related changes in cortical thickness, FA and MD were best represented with nonlinear fits, whereas for WM volume, linear fits best represented the data. Among the selected regions, the exception from this was the linear relation seen between FA and age in the medial orbitofrontal WM region. Note that for WM volume, gender was regressed out.

parietal lobe, followed by medial and superior regions in the frontal lobe, the cingulum and the occipital lobe. The estimated age at 90% of minimum cortical thickness exceeded the age range of the sample in many of the regions, indicating a protracted developmental course and/or a slow transition into the cortical dimensions of adulthood. Among the regions that reached 90% of their minimum cortical thickness earliest were the lateral occipital cortex and regions in the lateral orbitofrontal cortex. These regions have previously also been shown to reach the point where thickness increase gives way to decrease relatively early in development (Shaw et al. 2008). The relationship between timing of cortical thickening in late childhood and

timing of cortical thinning in adolescence and early adulthood is however not known and needs to be investigated more directly. We did not find any childhood increase in thickness in contrast to what has been reported in other developmental studies (Giedd et al. 1996; Shaw et al. 2008). Most likely our sample was too old to detect this early thickening. Shaw et al. (2008) included younger participants (age range 3.5–33 years) and found that peak cortical thickness was attained first in sensory areas at around 7 years of age and that almost the entire cortex had reached its peak thickness by 10.5 years of age. This is mainly consistent with our results exclusively showing cortical thinning in the second and third decades of life.

Table 5

Unique effects of cortical thickness, WM volume, and FA

Region	Cortical thickness		WM volume		FA		Model	
	β	sig β	β	sig β	β	sig β	R^2	F
Banks superior temporal sulcus	-0.59	0.000	0.24	0.000	0.20	0.001	0.51	57.72
Caudal anterior cingulate	-0.42	0.000	0.03	0.634	0.27	0.000	0.32	25.99
Caudal middle frontal	-0.57	0.000	0.13	0.028	0.22	0.000	0.46	47.23
Cuneus	-0.63	0.000	0.26	0.000	-0.15	0.006	0.57	71.47
Entorhinal	0.20	0.007	0.28	0.000	0.27	0.000	0.17	11.04
Fusiform	-0.56	0.000	0.19	0.001	0.14	0.014	0.49	51.55
Inferior parietal	-0.70	0.000	0.03	0.497	0.17	0.001	0.66	107.20
Inferior temporal	-0.44	0.000	0.04	0.448	0.42	0.000	0.54	63.89
Isthmus cingulate	-0.51	0.000	0.09	0.089	0.32	0.000	0.54	63.41
Lateral occipital	-0.62	0.000	0.07	0.251	0.19	0.002	0.55	66.78
Lateral orbitofrontal	-0.45	0.000	0.14	0.032	0.30	0.000	0.44	42.33
Lingual	-0.61	0.000	0.20	0.000	-0.21	0.000	0.56	68.96
Medial orbitofrontal	-0.61	0.000	0.05	0.407	-0.07	0.248	0.41	38.16
Middle temporal	-0.61	0.000	0.04	0.519	0.20	0.001	0.50	54.62
Parahippocampal	-0.08	0.206	0.17	0.006	0.57	0.000	0.43	40.74
Paracentral	-0.68	0.000	0.15	0.005	-0.06	0.238	0.57	70.90
Pars opercularis	-0.50	0.000	0.14	0.017	0.32	0.000	0.53	61.40
Pars orbitalis	-0.41	0.000	0.10	0.137	0.18	0.000	0.36	31.19
Pars triangularis	-0.61	0.000	0.05	0.379	0.21	0.000	0.50	54.75
Pericalcarine	-0.57	0.000	0.17	0.007	-0.16	0.016	0.44	43.29
Postcentral	-0.63	0.000	0.29	0.000	0.05	0.395	0.57	72.15
Posterior cingulate	-0.61	0.000	0.06	0.236	0.28	0.000	0.61	86.26
Precentral	-0.39	0.000	0.26	0.000	0.38	0.000	0.57	71.06
Precuneus	-0.71	0.000	0.19	0.000	-0.05	0.270	0.64	98.35
Rostral anterior cingulate	-0.64	0.000	-0.04	0.516	0.05	0.402	0.42	39.39
Rostral middle frontal	-0.43	0.000	0.04	0.503	0.41	0.000	0.57	71.43
Superior frontal	-0.70	0.000	0.10	0.074	-0.02	0.753	0.57	71.17
Superior parietal	-0.65	0.000	0.14	0.009	0.16	0.005	0.64	98.17
Superior temporal	-0.41	0.000	0.25	0.000	0.26	0.000	0.48	50.23
Supramarginal	-0.71	0.000	0.08	0.160	0.07	0.186	0.58	76.63
Frontal pole	-0.49	0.000	-0.02	0.827	0.08	0.259	0.25	17.77
Temporal pole	0.11	0.104	0.48	0.000	-0.18	0.009	0.26	18.88
Transverse temporal	-0.39	0.000	0.19	0.005	0.23	0.001	0.31	23.95

Note: Multiple regressions on age with cortical thickness, WM volume (with gender regressed out), and FA as independent variables. All models were significant at $P < 0.001$ (uncorrected) and $P < 0.05$ Bonferroni corrected. $df = 3, 164$.

Linear volume increases with age were found in the majority of the WM regions, although nonlinear increases with more rapid increase at young age were also found in about one-third of the regions. The mainly linear increase in WM volume is in general agreement with findings of previous studies (Giedd et al. 1999; Lebel et al. 2008) and demonstrates a less clear timing of developmental change in WM volume than for cortical thickness or diffusion parameters. Thus, as most cortical regions showed a nonlinear developmental pattern, in contrast to the tendency to linear WM volume development, it seems that the latter have a prolonged developmental course. This is coherent with studies of adults, showing WM volume growth until middle age (Allen et al. 2005; Walhovd et al. 2005). For the DTI data, our results are consistent with previous research showing anisotropy increase and overall diffusion decrease in WM continuing into adolescence and even early adulthood (Cascio et al. 2007; Lebel et al. 2008). In most regions, decelerating FA increase and MD decrease with age were observed. A cluster of regions in the medial posterior part of the brain did however surprisingly show linear decreases in FA with age, although of fairly small magnitude. The interpretation of this finding is unclear and needs to be replicated. Analyses of the eigenvalues suggest that the observed FA increase and MD decrease are mainly driven by decreases in DR, but that reductions in DA also contribute to the MD decrease to some extent. DR did however account for more of the FA and MD changes both in terms of size of effects

Table 6

Unique effects of cortical thickness, WM volume, and MD

Region	Cortical thickness		WM volume		MD		Model	
	β	sig β	β	sig β	β	sig β	R^2	F
Banks superior temporal sulcus	-0.63	0.000	0.25	0.000	-0.07	0.248	0.48	51.02
Caudal anterior cingulate	-0.48	0.000	0.01	0.870	-0.20	0.002	0.30	23.04
Caudal middle frontal	-0.51	0.000	0.14	0.012	-0.30	0.000	0.50	53.87
Cuneus	-0.66	0.000	0.22	0.000	0.01	0.825	0.55	65.90
Entorhinal	0.20	0.010	0.32	0.000	0.12	0.108	0.11	6.78
Fusiform	-0.57	0.000	0.20	0.001	-0.14	0.017	0.48	51.35
Inferior parietal	-0.80	0.000	0.03	0.525	0.02	0.713	0.64	97.53
Inferior temporal	-0.49	0.000	0.09	0.127	-0.34	0.000	0.51	55.96
Isthmus cingulate	-0.61	0.000	0.09	0.122	-0.16	0.007	0.48	50.47
Lateral occipital	-0.69	0.000	0.11	0.045	0.00	0.969	0.52	60.10
Lateral orbitofrontal	-0.48	0.000	0.12	0.074	-0.23	0.000	0.40	36.77
Lingual	-0.66	0.000	0.17	0.004	-0.10	0.064	0.53	60.38
Medial orbitofrontal	-0.52	0.000	0.03	0.565	-0.29	0.000	0.48	50.52
Middle temporal	-0.56	0.000	0.04	0.540	-0.25	0.000	0.51	57.72
Parahippocampal	-0.20	0.003	0.18	0.008	-0.46	0.000	0.34	27.90
Paracentral	-0.69	0.000	0.16	0.004	-0.04	0.468	0.56	70.23
Pars opercularis	-0.47	0.000	0.16	0.006	-0.31	0.000	0.52	58.27
Pars orbitalis	-0.36	0.000	0.14	0.040	-0.30	0.000	0.37	32.31
Pars triangularis	-0.54	0.000	0.06	0.275	-0.25	0.000	0.51	56.37
Pericalcarine	-0.63	0.000	0.13	0.043	-0.01	0.878	0.42	39.87
Postcentral	-0.61	0.000	0.28	0.000	-0.10	0.077	0.58	74.03
Posterior cingulate	-0.66	0.000	0.08	0.121	-0.22	0.000	0.60	80.39
Precentral	-0.37	0.000	0.30	0.000	-0.34	0.000	0.54	64.41
Precuneus	-0.71	0.000	0.20	0.000	-0.04	0.424	0.64	97.81
Rostral anterior cingulate	-0.64	0.000	-0.06	0.351	-0.12	0.039	0.43	41.46
Rostral middle frontal	-0.49	0.000	0.03	0.551	-0.32	0.000	0.52	59.65
Superior frontal	-0.61	0.000	0.12	0.043	-0.15	0.011	0.58	76.21
Superior parietal	-0.71	0.000	0.16	0.002	-0.02	0.621	0.63	91.11
Superior temporal	-0.45	0.000	0.23	0.000	-0.25	0.000	0.48	49.38
Supramarginal	-0.73	0.000	0.07	0.189	0.00	0.988	0.58	75.23
Frontal pole	-0.50	0.000	-0.03	0.708	0.03	0.718	0.25	17.58
Temporal pole	0.10	0.133	0.47	0.000	0.10	0.151	0.23	16.74
Transverse temporal	-0.36	0.000	0.17	0.008	-0.33	0.000	0.36	30.27

Note: Multiple regressions on age with cortical thickness, WM volume (with gender regressed out), and MD as independent variables. All models were significant at $P < 0.001$ (uncorrected) and $P < 0.05$ Bonferroni corrected. $df = 3, 164$.

and number of regions with significant change with age. Although many factors most likely influence the different diffusion parameters, studies on mice by Song et al. (2002, 2003, 2005) indicate that degree of myelination is one important factor for DR, but not DA. Our results therefore indirectly indicate continued myelination of fiber tracts during adolescence and even well into the twenties, which fits well with results from post mortem studies (Yakovlev and Lecours 1967; Benes 1989; Benes et al. 1994). We also found regional differences in the developmental timing of the diffusion parameters. FA and MD in major tracts in the frontal and temporal lobes reach their developmental plateau later than in other regions. This supports previous studies reporting that tracts with fronto-temporal connections tend to mature more slowly than others (Schneiderman et al. 2007; Lebel et al. 2008). Our results further show this pattern of late maturation of tracts in the frontal and temporal lobes with a more differentiated regional approach.

Knowledge about the maturation of both the cerebral cortex and WM has implications for the understanding of cognitive development. Although it is well established that brain maturation and cognitive development occur concurrently during childhood and adolescence (Casey et al. 2005; Schmithorst et al. 2005; Durston and Casey 2006; Shaw et al. 2006), the relationship remains unclear. Questions further remain concerning the relative roles of the various observed structural cerebral changes in cognitive development.

Table 7
Associations between cortical thickness and WM in development

Region	WM volume	FA	MD	DA	DR
Banks superior temporal sulcus	0.02	-0.28	0.24	0.01	0.28
Caudal anterior cingulate	-0.15	-0.31	0.11	-0.20	0.23
Caudal middle frontal	-0.12	-0.18	0.34	0.34	0.30
Cuneus	-0.22	0.14	0.11	0.21	-0.01
Entorhinal	-0.26	-0.06	-0.03	-0.07	0.01
Fusiform	-0.32	-0.22	0.17	-0.01	0.25
Inferior parietal	-0.29	-0.51	0.25	-0.17	0.41
Inferior temporal	-0.29	-0.42	0.31	-0.10	0.41
Isthmus cingulate	-0.14	-0.45	0.28	-0.22	0.46
Lateral occipital	-0.27	-0.42	0.07	-0.26	0.27
Lateral orbitofrontal	-0.47	-0.23	0.19	-0.02	0.24
Lingual	-0.23	0.20	-0.08	0.06	-0.21
Medial orbitofrontal	-0.28	0.10	0.37	0.42	0.21
Middle temporal	-0.25	-0.27	0.42	0.19	0.40
Parahippocampal	-0.13	-0.26	0.06	-0.20	0.17
Paracentral	-0.23	0.26	0.18	0.43	-0.13
Pars opercularis	-0.34	-0.31	0.40	0.27	0.38
Pars orbitalis	-0.31	-0.29	0.40	0.26	0.40
Pars triangularis	-0.32	-0.22	0.45	0.46	0.40
Pericalcarine	-0.06	0.39	-0.19	0.03	-0.28
Postcentral	-0.22	-0.23	0.34	0.26	0.35
Posterior cingulate	-0.14	-0.42	0.28	-0.17	0.39
Precentral	-0.029	-0.23	0.29	0.27	0.27
Precuneus	-0.28	0.21	0.31	0.43	0.10
Rostral anterior cingulate	-0.25	-0.19	0.13	-0.08	0.20
Rostral middle frontal	-0.30	-0.54	0.50	0.22	0.54
Superior frontal	-0.45	-0.02	0.52	0.60	0.36
Superior parietal	-0.37	-0.49	0.13	-0.25	0.34
Superior temporal	-0.29	-0.42	0.32	-0.02	0.41
Supramarginal	-0.35	-0.33	0.41	0.25	0.43
Frontal pole	0.02	-0.09	0.05	0.02	0.07
Temporal pole	-0.05	-0.05	0.15	0.13	0.12
Transverse temporal	-0.19	-0.14	0.19	0.10	0.18

Note: Correlations between cortical thickness and WM volume (with gender regressed out), FA, MD, DA, and DR. Bold characters indicate $P < 0.05$ uncorrected and underlined indicate $P < 0.05$ Bonferroni corrected $N = 168$.

Relationships between Age-Related Changes in Cortical Thickness, WM Volume, and DTI

Development of cortical GM, WM volume, and WM diffusion parameters have never before been investigated across the brain in the same sample. Knowledge about the relationships between these developmental changes is important for gaining a better understanding of the complex processes of brain maturation, and this was the main aim of the present study. The results demonstrated unique relations between age and cortical thickness, WM volume, and diffusion properties. This observation indicates that different maturational processes are at play in different tissue classes simultaneously. Of the 3 classes of measures, cortical thickness was clearly the measure most strongly related to age. An important question regards whether cortical GM development drives WM development. As mentioned, the present data show stronger relationships between age and cortical thickness than between age and WM volume or DTI parameters. Still, longitudinal data from earlier in life are needed to give more definite conclusions.

The present data provide some indirect information about possible neurobiological processes involved in brain development. The relations between age and regional cortical thickness remained strong even when controlling for the influence of underlying WM volume and diffusion measures. Hence, the observed age-related cortical thinning is therefore likely not explained by WM maturation in underlying regions alone. This provides indirect evidence for the view that the measured cortical thinning is not exclusively an effect of lower

cortical layers changing classification from GM to WM due to increased myelination in the underlying WM. Age-related changes of diffusion parameters in cortical regions were however not investigated, leaving increased myelination of cortico-cortical fibers unaccounted for as a possible factor that might influence measures of cortical thickness.

Based on a study combining cortical morphometry and electroencephalography (EEG), Whitford et al. (2007) suggest that the age-related reduction in EEG power is attributable to an elimination of active synapses and that the cortical changes might reflect pruning-associated reduction of neuropil. However, Bourgeois and Rakic (1993) and Paus et al. (2008) pointed out that it is unlikely that a decrease in synaptic density per se can explain the observed cortical thinning and volume reductions in adolescence because the total volume of synaptic boutons is of a much smaller scale. A reduction in number of synapses might, however, in addition to a reduction in neuropil, also be accompanied by a reduction in the number of glial cells that together could account for cortical thickness and volume changes (Paus et al. 2008). More direct evidence of the processes that underlie the reported changes in cerebral cortex and WM during adolescence is needed to expand the current findings. Quantitative histological studies are likely required to really understand the neurobiology involved in the apparent cortical thinning. In vivo MRI and DTI have the potential to track changes over time and combined with more direct evidence from histological studies, this might greatly improve our understanding of brain maturation.

Associations between Cortical Thickness and WM Properties in Development

The present study is the first to report regional correlations between cortical thickness and WM properties across the brain in development. Associated age-related changes in cortex and underlying WM could conceivably be expected to occur as a consequence of experience-dependent regional development in which development of cortical areas is either dependent on or drives development in underlying connected tracts. Alternatively, associated changes might be expected resulting from genetic preprogramming of neural networks involving both cortical areas and connecting tracts. In short, we found negative correlations between cortical thickness and WM volume in most regions studied. Cortical thickness correlated negatively with FA in about two-thirds of the underlying regions and positively with a cluster of regions in the medial posterior part of the brain. Positive correlations between cortical thickness and MD were found in about two-thirds of the regions. The median correlations between the different measures were of medium effect size. Giorgio et al. (2008) have previously reported a strong correlation of -0.65 between GM density in a cluster in the right frontal lobe and FA in the connected superior part of the corona radiata. Based on this correlation they suggested that associated age-related changes may be occurring in cortex and WM microstructure. In some ways, our results support this conclusion, with significant, although somewhat weaker, negative correlations between cortical thickness and FA in underlying tracts. However, the pattern of age-related changes does seem to diverge to a substantial extent between the different measures studied. This is evident from Figure 4. The most prominent relative age-related cortical thinning was found in parietal lobe regions.

Besides deep WM, the largest relative volume increases in WM were found in regions distributed in all the lobes, including regions in the temporal and frontal lobes with relatively little cortical thinning. In contrast, the largest percentage increases in FA were spread in lateral regions in all lobes as well as in the cingulum regions, whereas large relative decreases in MD were found in the frontal, temporal, and medial parietal lobes. Our results do therefore not indicate a regionally tightly linked pattern of age-related changes in cortical thickness and underlying WM properties. This means that regional cortical development only to a moderate degree is descriptive of WM development measured by volumetry or DTI.

Limitations and Conclusions

As this is the first study to investigate regional relationships between cortical and WM volume and microstructure development in the same sample, the results from these analyses should be replicated, preferably in longitudinal studies, as there are serious challenges involved in drawing inferences about longitudinal processes from cross-sectional studies with unknown age-related recruitment bias (Kraemer et al. 2000). The diffusion metrics used in the present study were sampled from areas presumably included in major WM fiber tracts. In order to further explore the relationships between GM and WM in development, future studies should sample areas in closer proximity to this boundary. However, one challenge with such an approach is that more crossing fibers will likely be sampled and anisotropy might be severely underestimated. The approach in the present study was employed in order to minimize this threat. The present sample showed relatively high cognitive function and may not be seen as representative of the full range of individual differences in development. Further, a more detailed investigation of possible sex differences could have been conducted as several previous studies have reported such differences during brain development (Giedd et al. 1999; Lenroot et al. 2007; Schneiderman et al. 2007; Sowell et al. 2007; Schmithorst et al. 2008). When controlling for brain size, findings of sex differences in cortical GM in both adults and children have been inconsistent, with some studies reporting no difference, and some showing enlargements in females (Sowell et al. 2007). Findings have also been inconsistent with respect to interactions between age and sex in measures of regional brain volumes. Possible laterality effects could also have been investigated further, as asymmetry of GM, WM, and anisotropy have been reported in previous studies on adults (Good et al. 2001; Watkins et al. 2001; Büchel et al. 2004; Gong et al. 2005). We did not find any main effects of sex except for on WM volume, where sex therefore was regressed out, nor any interaction effects between age and sex nor age and hemisphere for any of the measures. Sex and hemisphere were therefore combined for all of our analyses in order to simplify interpretation, ensure high statistical power, and improve curve fits. Future studies could however investigate both sex differences and laterality effects during brain development in greater detail. The effects of steroid hormones on sexual dimorphisms in both cortical and subcortical maturation could also be studied further (Neufang et al. 2009).

In conclusion, we found regional age-related cortical thinning, WM volume increases, and changes in diffusion parameters in major tracts in a sample of 168 healthy participants between 8 and 30 years. All 3 classes of measures were sensitive to brain

maturation, showing unique associations with age, although cortical thickness was the most strongly age-related parameter. Thus, inclusion of both morphometry and DTI in studies of brain maturation will likely enhance our understanding. The results further indicate that cortical thinning in adolescence cannot be fully explained by WM maturation in adjacent areas as measured by volumetry or DTI in major tracts. Although MRI and DTI studies are unable to be directly informative on the neurobiological processes underlying brain maturation, this finding may implicate that proliferation of myelin into the periphery of the cortical neuropil is not likely the sole factor accounting for the observed cortical thinning during adolescence.

Changing imaging properties of different cerebral tissues may potentially reflect multiple processes influencing differences in tissue contrast; caution is warranted when interpreting these results with respect to specific neurobiological processes. We also found medium sized correlations between cortical thickness and both volume and diffusion parameters in underlying WM regions in development, although there did not seem to be any strong regional relationships between cortical and WM maturation.

Supplementary Material

Supplementary Figure 1, Supplementary Movie 1, and Supplementary Tables 1–11 can be found at: <http://www.cercor.oxfordjournals.org/>

Funding

Norwegian Research Council (177404/W50 and 186092/V50 to K.B.W., 170837/V50 to Ivar Reinvang); The University of Oslo (to K.B.W.); and the Department of Psychology, University of Oslo (to A.M.F.).

Notes

The authors would like to thank Mari Torstveit and Victoria Torp Sells for their effort in the data collection and Inge Amlien for making the Supplementary movie. We would also like to thank all the participants and the children's parents. *Conflict of Interest:* None declared.

Address correspondence to email: c.k.tamnes@psykologi.uio.no.

References

- Allen JS, Bruss J, Brown CK, Damasio H. 2005. Normal neuroanatomical variation due to age: the major lobes and a parcellation of the temporal region. *Neurobiol Aging*. 26:1245–1260.
- Ashtari M, Cervellione KL, Hasan KM, Wu J, McIlree C, Kester H, Ardekani BA, Roofeh D, Szeszko PR, Kumra S. 2007. White matter development during late adolescence in healthy males: a cross-sectional diffusion imaging study. *Neuroimage*. 35:501–510.
- Barnea-Goraly N, Menon V, Eckert M, Tamm L, Bammner R, Karchemskiy A, Dant CC, Reiss AL. 2005. White matter development during childhood and adolescence: a cross-sectional diffusion tensor imaging study. *Cereb Cortex*. 15:1848–1854.
- Bartzokis G, Beckson M, Lu PO, Nuechterlein KH, Edwards N, Mintz J. 2001. Age-related changes in frontal and temporal lobe volumes in men. *Arch Gen Psychiatry*. 58:461–465.
- Beaulieu C. 2002. The basis of anisotropic water diffusion in the nervous system—a technical review. *NMR Biomed*. 15:435–455.
- Ben Bashat D, Ben Sira L, Graif M, Pianka P, Hendler T, Cohen Y, Assaf Y. 2005. Normal white matter development from infancy to adulthood: comparing diffusion tensor and high *b* value diffusion weighted MR images. *J Magn Reson Imaging*. 21:503–511.
- Benes FM. 1989. Myelination of cortical-hippocampal relays during late adolescence. *Schizophr Bull*. 15:585–593.

- Benes FM, Turtle M, Khan Y, Farol P. 1994. Myelination of a key relay zone in the hippocampal formation occurs in the human brain during childhood, adolescence, and adulthood. *Arch Gen Psychiatry*. 51:477-484.
- Bonekamp D, Nagae LM, Degaonker M, Matson M, Abdalla WMA, Barker PB, Mori S, Horska A. 2007. Diffusion tensor imaging in children and adolescents: reproducibility, hemispheric, and age-related differences. *Neuroimage*. 34:733-742.
- Bourgeois JP, Rakic P. 1993. Changes of synaptic density in the primary visual cortex of the macaque monkey from fetal to adult stage. *J Neurosci*. 13:2801-2820.
- Büchel C, Raedler T, Sommer M, Sach M, Weiller C, Koch MA. 2004. White matter asymmetry in the human brain: a diffusion tensor MRI study. *Cereb Cortex*. 14:945-951.
- Cascio CJ, Gerig G, Piven J. 2007. Diffusion tensor imaging: application to the study of the developing brain. *J Am Acad Child Adolesc Psychiatry*. 46:213-223.
- Casey BJ, Tottenham N, Liston C, Durston S. 2005. Imaging the developing brain: what have we learned about cognitive development? *Trends Cogn Sci*. 9:104-110.
- Courchesne E, Chisum HJ, Townsend J, Cowles A, Covington J, Egaas B, Harwood M, Hinds S, Press GA. 2000. Normal brain development and aging: quantitative analysis at in vivo MR imaging in healthy volunteers. *Neuroradiology*. 216:672-682.
- Dale AM, Fischl B, Sereno MI. 1999. Cortical surface-based analysis. I. Segmentation and surface reconstruction. *Neuroimage*. 9:179-194.
- Dale AM, Sereno MI. 1993. Improved localization of cortical activity by combining EEG and MEG with MRI cortical surface reconstruction: a linear approach. *J Cogn Neurosci*. 5:162-176.
- Desikan RS, Segonne F, Fischl B, Quinn BT, Dickerson BC, Blacker D, Buckner RL, Dale AM, Maguire RP, Hyman BT, et al. 2006. An automated labeling system for subdividing the human cerebral cortex on MRI scans into gyral based regions of interest. *Neuroimage*. 31:968-980.
- Durston S, Casey BJ. 2006. What have we learned about cognitive development from neuroimaging? *Neuropsychologia*. 44:2149-2157.
- Eluvathingal TJ, Hasan KM, Kramer L, Fletcher JM, Ewing-Cobbs L. 2007. Quantitative diffusion tensor tractography of association and projection fibres in normally developing children and adolescents. *Cereb Cortex*. 17:2760-2768.
- Fischl B, Dale AM. 2000. Measuring the thickness of the human cerebral cortex from magnetic resonance images. *Proc Natl Acad Sci USA*. 97:11050-11055.
- Fischl B, Liu A, Dale AM. 2001. Automated manifold surgery: constructing geometrically accurate and topologically correct models of the human cerebral cortex. *IEEE Trans Med Imaging*. 20:70-80.
- Fischl B, Sereno MI, Dale AM. 1999a. Cortical surface-based analysis. II: inflation, flattening, and a surface-based coordinate system. *Neuroimage*. 9:195-207.
- Fischl B, Sereno MI, Tootell RBH, Dale AM. 1999b. High-resolution intersubject averaging and a coordinate system for the cortical surface. *Hum Brain Mapp*. 8:272-284.
- Fischl B, van der Kouwe A, Destrieux C, Halgren E, Segonne F, Salat DH, Busa E, Seidman LJ, Goldstein J, Kennedy D, et al. 2004. Automatically parcellating the human cerebral cortex. *Cereb Cortex*. 14:11-22.
- Fjell AM, Westlye LT, Greve DN, Fischl B, Benner T, van der Kouwe AJW, Salat D, Bjørnerud A, Due-Tønnessen P, Walhovd KB. 2008. The relationship between diffusion tensor imaging and volumetry as measures of white matter properties. *Neuroimage*. 42:1654-1668.
- Giedd JN. 2004. Structural magnetic resonance imaging of the adolescent brain. *Ann NY Acad Sci*. 1021:77-85.
- Giedd JN, Blumenthal J, Jeffries NO, Castellanos FX, Liu H, Zijdenbos A, Paus T, Evans AC, Rapoport JL. 1999. Brain development during childhood and adolescence: a longitudinal MRI study. *Nat Neurosci*. 2:861-863.
- Giedd JN, Snell JW, Lange N, Rajapakse JC, Casey BJ, Kozuch PL, Vaituzis AC, Vauss YC, Hamburger SD, Kaysen D, et al. 1996. Quantitative magnetic resonance imaging of human brain development: ages 4-18. *Cereb Cortex*. 6:551-560.
- Giorgio A, Watkins KE, Douaud G, James AC, James S, De Stefano N, Matthews PM, Smith SM, Johansen-Berg H. 2008. Changes in white matter microstructure during adolescence. *Neuroimage*. 39:52-61.
- Gogtay N, Giedd JN, Lusk L, Hayashi KM, Greenstein D, Vaituzis AC, Nugent TF, III, Herman DH, Clasen LS, Toga AW, et al. 2004. Dynamic mapping of human cortical development during childhood through early adulthood. *Proc Natl Acad Sci*. 101:8174-8179.
- Gong G, Jiang T, Zhu C, Zang Y, He Y, Xie S, Xiao J. 2005. Side and handedness effects on the cingulum from diffusion tensor imaging. *Neuroreport*. 16:1701-1705.
- Good CD, Johnsrude I, Ashburner J, Henson RNA, Friston KJ, Frackowiak RSJ. 2001. Cerebral asymmetry and the effects of sex and handedness on brain structure: a voxel-based morphometric analysis of 465 normal adult human brains. *Neuroimage*. 14:685-700.
- Hensch TK. 2004. Critical period regulation. *Annu Rev Neurosci*. 27:549-579.
- Hua K, Zhang J, Wakana S, Jiang H, Li X, Reich DS, Calabresi PA, Pekar JJ, van Zijl PCM, Mori S. 2008. Tract probability maps in stereotaxic spaces: analyses of white matter anatomy and tract-specific quantifications. *Neuroimage*. 39:336-347.
- Huttenlocher PR, Dabholkar AS. 1997. Regional differences in synaptogenesis in human cerebral cortex. *J Comp Neurol*. 387:167-178.
- Jenkinson M, Smith S. 2001. A global optimisation method for robust affine registration of brain images. *Med Image Anal*. 5:143-156.
- Jernigan TL, Trauner DA, Hesselink JR, Tallal PA. 1991. Maturation of human cerebrum observed in vivo during adolescence. *Brain*. 114:2037-2049.
- Kennedy DN, Makris N, Herbert MR, Takahashi T, Caviness VS. 2002. Basic principles of MRI morphometry studies of human brain development. *Dev Sci*. 5:268-278.
- Klingberg T, Vaidya CJ, Gabrieli JDE, Moseley ME, Hedehus M. 1999. Myelination and organization of the frontal white matter in children: diffusion tensor MRI study. *Neuroreport*. 10:2817-2821.
- Knudsen EI. 2004. Sensitive periods in the development of the brain and behavior. *J Cogn Neurosci*. 16:1412-1425.
- Kraemer HC, Yesavage JA, Taylor JL, Kupfer D. 2000. How can we learn about developmental processes from cross-sectional studies, or can we? *Am J Psychiatry*. 157:163-171.
- Kuperberg GR, Broome MR, McGuire PK, David AS, Eddy M, Ozawa F, Goff D, West WC, Williams SCR, van der Kouwe AJW, et al. 2003. Regionally localized thinning of the cerebral cortex in schizophrenia. *Arch Gen Psychiatry*. 60:878-888.
- Lebel C, Walker L, Leemans A, Phillips L, Beaulieu C. 2008. Microstructural maturation of the human brain from childhood to adulthood. *Neuroimage*. 40:1044-1055.
- Le Bihan D. 2003. Looking into the functional architecture of the brain with diffusion MRI. *Nat Rev Neurosci*. 4:469-480.
- Lenroot RK, Gogtay N, Greenstein DK, Wells EM, Wallace GL, Clasen LS, Blumenthal JD, Lerch J, Zijdenbos AP, Evans AC, et al. 2007. Sexual dimorphism of brain developmental trajectories during childhood and adolescence. *Neuroimage*. 36:1065-1073.
- Mori S, Wakana S, Nagae-Poetscher LM, van Zijl PCM. 2005. MRI atlas of human white matter. Amsterdam (The Netherlands): Elsevier.
- Mori S, Zhang J. 2006. Principles of diffusion tensor imaging and its applications to basic neuroscience research. *Neuron*. 51:527-539.
- Morriss MC, Zimmerman RA, Bilaniuk LT, Hunter JV, Haselgrove JC. 1999. Changes in brain water diffusion during childhood. *Neuroradiology*. 41:929-934.
- Mukherjee P, Miller JH, Shimony JS, Conturo TE, Lee BCP, Almlí CR, McKinstry RC. 2001. Normal brain maturation during childhood: developmental trends characterized with diffusion-tensor MR imaging. *Radiology*. 221:349-358.
- Mukherjee P, Miller JH, Shimony JS, Philip JV, Nehra D, Snyder AZ, Conturo TE, Neil JJ, McKinstry RC. 2002. Diffusion-tensor MR imaging of grey and white matter development during normal human brain maturation. *Am J Neuroradiol*. 23:1445-1456.
- Neufang S, Specht K, Hausmann M, Güntürkün O, Herpertz-Dahlmann B, Fink GR, Konrad K. 2009. Sex differences and the impact of steroid hormones on the developing human brain. *Cereb Cortex*. 19:464-473.

- Paus T, Collins DL, Evans AC, Leonard G, Pike B, Zijdenbos A. 2001. Maturation of white matter in the human brain: a review of magnetic resonance studies. *Brain Res Bull.* 54:255-266.
- Paus T, Keshavan M, Giedd JN. 2008. Why do many psychiatric disorders emerge during adolescence? *Nat Rev Neurosci.* 9:947-957.
- Pfefferbaum A, Mathalon DH, Sullivan EV, Rawles JM, Zipursky RB, Lim KO. 1994. A quantitative magnetic resonance imaging study of changes in brain morphology from infancy to late adulthood. *Arch Neurol.* 51:874-887.
- Pierpaoli C, Basser PJ. 1996. Toward a quantitative assessment of diffusion anisotropy. *Magn Reson Med.* 36:893-906.
- Qiu D, Tan LH, Zhou K, Khong PL. 2008. Diffusion tensor imaging of normal white matter maturation from late childhood to young adulthood: voxel-wise evaluation of mean diffusivity, fractional anisotropy, radial and axial diffusivity, and correlation with reading development. *Neuroimage.* 41:223-232.
- Reese TG, Heid O, Weisskoff RM, Wedeen VJ. 2003. Reduction of eddy-current-induced distortion in diffusion MRI using a twice-refocused spin echo. *Magn Reson Med.* 49:177-182.
- Reiss AL, Abrams MT, Singer HS, Ross JL, Denckla MB. 1996. Brain development, gender and IQ in children. A volumetric imaging study. *Brain.* 119:1763-1774.
- Rivkin MJ. 2000. Developmental neuroimaging of children using magnetic resonance techniques. *Ment Retard Dev Disabil Res Rev.* 6:68-80.
- Rosas HD, Liu AK, Hersch S, Glessner M, Ferrante RJ, Salat DH, van der Kouwe A, Jenkins BG, Dale AM, Fischl B. 2002. Regional and progressive thinning of the cortical ribbon in Huntington's disease. *Neurology.* 58:695-701.
- Salat DH, Buckner RL, Snyder AZ, Greve DN, Desikan RSR, Busa E, Morris JC, Dale AM, Fischl B. 2004. Thinning of the cerebral cortex in aging. *Cereb Cortex.* 14:721-730.
- Salat DH, Greve DN, Pacheco JL, Quinn BT, Helmer KG, Buckner RL, Fischl B. 2009. Regional white matter volume differences in nondemented aging and Alzheimer's disease. *Neuroimage.* 44:1247-1258.
- Schmithorst VJ, Holland SK, Dardzinski BJ. 2008. Developmental differences in white matter architecture between boys and girls. *Hum Brain Mapp.* 29:696-710.
- Schmithorst VJ, Wilke M, Dardzinski BJ, Holland SK. 2002. Correlation of white matter diffusivity and anisotropy with age during childhood and adolescence: a cross-sectional diffusion-tensor MR imaging study. *Radiology.* 222:212-218.
- Schmithorst VJ, Wilke M, Dardzinski BJ, Holland SK. 2005. Cognitive functions correlate with white matter architecture in a normal pediatric population: a diffusion tensor MRI study. *Hum Brain Mapp.* 26:139-147.
- Schneider JFL, Il'yasov KA, Henning J, Martin E. 2004. Fast quantitative diffusion-tensor imaging of cerebral white matter from the neonatal period to adolescence. *Neuroradiology.* 46:258-266.
- Schneiderman JS, Buchsbaum MS, Haznedar MM, Hazlett EA, Brickman AM, Schiabuuddin L, Brand JG, Totosjan Y, Newmark RE, Tang C, et al. 2007. Diffusion tensor anisotropy in adolescents and adults. *Neuropsychobiology.* 55:96-111.
- Segonne F, Dale AM, Busa E, Glessner M, Salat D, Hahn HK, Fischl B. 2004. A hybrid approach to the skull stripping problem in MRI. *Neuroimage.* 22:1060-1075.
- Segonne F, Grimson E, Fischl B. 2005. A genetic algorithm for the topology correction of cortical surfaces. *Inf Process Med Imaging.* 19:393-405.
- Shaw P, Greenstein D, Lerch J, Clasen L, Lenroot R, Gogtay N, Evans A, Rapoport J, Giedd J. 2006. Intellectual ability and cortical development in children and adolescents. *Nature.* 440:676-679.
- Shaw P, Kabani NJ, Lerch JP, Eckstrand K, Lenroot R, Gogtay N, Greenstein D, Clasen L, Evans A, Rapoport JL, et al. 2008. Neurodevelopmental trajectories of the human cerebral cortex. *J Neurosci.* 28:3586-3594.
- Smith SM, Jenkinson M, Woolrich MW, Beckmann CF, Behrens TEJ, Johansen-Berg H, Bannister PR, De Luca M, Drobnjak I, Flitney DE, et al. 2004. Advances in functional and structural MR image analysis and implementation as FSL. *Neuroimage.* 23:S208-S219.
- Snook L, Paulson LA, Roy D, Phillips L, Beaulieu C. 2005. Diffusion tensor imaging of neurodevelopment in children and young adults. *Neuroimage.* 26:1164-1173.
- Song SK, Sun SW, Ju WK, Lin SJ, Cross AH, Neufeld AH. 2003. Diffusion tensor imaging detects and differentiates axon and myelin degeneration in mouse optic nerve after retinal ischemia. *Neuroimage.* 20:1714-1722.
- Song SK, Sun SW, Ramsbottom MJ, Chang C, Russel J, Cross AH. 2002. Demyelination revealed through MRI as increased radial (but unchanged axial) diffusion of water. *Neuroimage.* 17:1429-1436.
- Song SK, Yoshino J, Le TQ, Lin SJ, Sun SW, Cross AH, Armstrong RC. 2005. Demyelination increases radial diffusivity in corpus callosum of mouse brain. *Neuroimage.* 26:132-140.
- Sowell ER, Peterson BS, Kan E, Woods RP, Yoshii J, Bansal R, Xu D, Zhu H, Thompson PM, Toga AW. 2007. Sex differences in cortical thickness mapped in 176 healthy individuals between 7 and 87 years of age. *Cereb Cortex.* 17:1550-1560.
- Sowell ER, Peterson BS, Thompson PM, Welcome SE, Henkenius AL, Toga AW. 2003. Mapping cortical change across the human life span. *Nat Neurosci.* 6:309-315.
- Sowell ER, Thompson PM, Leonard CM, Welcome SE, Kan E, Toga AW. 2004. Longitudinal mapping of cortical thickness and brain growth in normal children. *J Neurosci.* 24:8223-8231.
- Sowell ER, Trauner DA, Gamst A, Jernigan TL. 2002. Development of cortical and subcortical brain structures in childhood and adolescence: a structural MRI study. *Dev Med Child Neurol.* 44:4-16.
- Suzuki Y, Matsuzawa H, Kwee IL, Nakada T. 2003. Absolute eigenvalue diffusion tensor analysis for human brain maturation. *NMR Biomed.* 16:257-260.
- Wakana S, Caprihan A, Panzenboeck MM, Fallon JH, Perry M, Gollub RL, Hua K, Zhang J, Jiang H, Dubey P, et al. 2007. Reproducibility of quantitative tractography methods applied to cerebral white matter. *Neuroimage.* 36:630-644.
- Walhovd KB, Fjell AM, Reinvang I, Lundervold A, Dale AM, Eilertsen DE, Quinn BT, Salat D, Makris N, Fischl B. 2005. Effects of age on volumes of cortex, white matter and subcortical structures. *Neurobiol Aging.* 26:1261-1270.
- Watkins KE, Paus T, Lerch JP, Zijdenbos A, Collins DL, Neelin P, Taylor J, Worsley KJ, Evans AC. 2001. Structural asymmetries in the human brain: a voxel-based statistical analysis of 142 MRI scans. *Cereb Cortex.* 11:868-877.
- Wechsler D. 1999. Wechsler Abbreviated Scale of Intelligence (WASI). San Antonio (TX): The Psychological Corporation.
- Westlye LT, Walhovd KB, Bjørnerud A, Due-Tønnesen P, Fjell AM. 2009. Error-related negativity is mediated by fractional anisotropy in the posterior cingulate gyrus—a study combining diffusion tensor imaging and electrophysiology in healthy adults. *Cereb Cortex.* 19:293-304.
- Whitford TJ, Rennie CJ, Grieve SM, Clark CR, Gordon E, Williams LM. 2007. Brain maturation in adolescence: concurrent changes in neuroanatomy and neurophysiology. *Hum Brain Mapp.* 28:228-237.
- Wozniak JR, Lim KO. 2006. Advances in white matter imaging: a review of in vivo magnetic resonance methodologies and their applicability to the study of development and aging. *Neurosci Biobehav Rev.* 30:762-774.
- Yakovlev PI, Lecours AR. 1967. The myelogenetic cycles of regional maturation of the brain. In: Minkowski A, editor. *Regional development of the brain early in life.* Boston (MA): Blackwell Scientific Publications Inc. p. 3-70.
- Zhang L, Thomas KM, Davidson MC, Casey BJ, Heier LA, Ulug AM. 2005. MR quantitation of volume and diffusion changes in the developing brain. *Am J Neuroradiol.* 26:45-49.